A Study of Minimax Access-Point Setup Optimization Approach in IEEE 802.11n Wireless Local-Area Network

September, 2018

Kyaw Soe Lwin

Graduate School of
Natural Science and Technology

(Doctor's Course)
Okayama University

Dissertation submitted to
Graduate School of Natural Science and Technology
of
Okayama University
for
partial fulfillment of the requirements
for the degree of
Doctor of Philosophy.

Written under the supervision of

Professor Nobuo Funabiki

and co-supervised by
Professor Satoshi Denno
and
Professor Yasuyuki Nogami

Okayama University, September 2018.

To Whom It May Concern

We hereby certify that this is a typical copy of the original doctor thesis of
Mr. Kyaw Soe Lwin

Signature of

the Supervisor

Prof. Nobuo Funabiki

Seal of

Graduate School of

Natural Science and Technology

Abstract

As a flexible and cost-efficient Internet access network, the *IEEE 802.11 wireless local-area network (WLAN)* has been broadly deployed around the world. Among several protocols, currently, *IEEE 802.11n* has prevailed over the *WLAN* due to high-speed data transmissions using the *channel bonding*, the *frame aggregation* and the *multiple input multiple output (MIMO)*. It has been observed that the signal propagation from an IEEE 802.11n *access-point (AP)* is not uniform in the circumferential and vertical directions. As a result, the data transmission speed between the AP and a host could be significantly affected by their relative setup conditions. Therefore, the optimal setup of each AP in the network field is significant to improve the performance of WLAN, whereas the setup of a host cannot be controlled by the network manager.

In this thesis, first, to investigate the significance of the AP setup optimization, we present throughput measurement results under various conditions in the placement height and orientation of an AP both in outdoor and indoor environments. The results show that throughput is greatly affected by the height and orientation of the AP due to the non-uniformity of the signal radiation along the horizontal and vertical planes, and confirm the significance of the AP setup optimization.

Next, we propose the *minimax AP setup optimization approach* to improve the throughput performance of WLAN. In this approach, we first detect a *bottleneck host* that receives the weakest signal from the AP in the field using the *throughput estimation model*. Then, we optimize the AP setup by changing the height and the orientation to maximize the throughput of this bottleneck host against the AP. In a real network field, the *coordinate of AP* can be slightly shifted, which may improve the *multipath effect* due to the complex structure of a building. Thus, we also optimize the *coordinate* of the AP setup as another optimization parameter.

In the proposed approach, the accurate throughput estimation model is critical to detect a bottleneck host in the network field correctly. For this goal, we present the *throughput estimation model* that consists of the *log-distance path loss model* and the *sigmoid function*. The first model estimates the *receiving signal strength (RSS)* at the receiving node. The second function converts RSS to the throughput. Besides, to further improve the accuracy in the field with several rooms, we introduce the simple model for the *multipath effect*.

The throughput estimation model in this thesis has several parameters whose values may be different depending on the network field and can determine the accuracy of the estimated throughput. To find the optimal values of the parameters from the measurement results, we present the *parameter optimization tool*, which can be used for various applications in addition to the throughput estimation model. It seeks the optimal values of the parameters such that the total error between the measured and estimated throughputs is minimized. With using this model, we present the *throughput measurement minimization procedure* to minimize the number of throughput measurement points to reduce the labor cost. It selects the limited host locations for throughput measurements to optimize the parameter values while keeping the accuracy.

Finally, we evaluate the accuracy of the throughput estimation model with the parameter op-

timization tool by comparing the measured and estimated throughputs in the three network fields. The same bottleneck host is found by the model and measurements for any AP location. Then, we evaluate the minimax AP setup optimization approach through extensive measurements in three network fields, and confirm the effectiveness of this proposal.

In future studies, we will apply the minimax AP setup optimization approach for other network fields, and extend the throughput estimation model to consider multiple APs and multiple hosts.

Acknowledgements

It is my great pleasure to thank those who have supported and encouraged me throughout my Ph.D. degree. It would not have been possible to complete this thesis without your helps. I want to say so much, but I can hardly find the words. So, I'll just say that you are the greatest blessing in my life.

I owe my deepest gratitude to my supervisor, Professor Nobuo Funabiki, who has supported me throughout my thesis with his patience and knowledge. I am greatly indebted to him, whose encouragements, advices, and supports from the beginning enabled me to develop the understanding of this subject, not only in scientific but also in life. He gave me wonderful advices, comments, and guidance when writing papers and presenting them. Thanks for making me what I am today.

I am deeply grateful to my co-supervisors, Professor Satoshi Denno and Professor Yasuyuki Nogami, for their continuous supports, guidance, and proofreading of this work.

I wish to express my sincere gratitude to Associate Professor Minoru Kuribayashi for his valuable suggestions during my research. I also want to express my gratitude to the course teachers during my Ph.D. study for enlightening me with wonderful knowledge.

I would like to acknowledge Japan International Cooperation Agency (JICA) for financially supporting my doctoral course study in Okayama University and to Yangon Technological University (YTU), where I was working as an Associate Professor, for allowing me to study abroad.

I would like to thank for the helpful discussions from many people including Dr. Md. Ezharul Islam, Dr. Chew Chang Choon, Dr. Nobuya Ishihara, Dr. Md. Selim Al Mamun, Dr. Khin Khin Zaw, Mr. Chihiro Taniguchi, Mr. Sumon Kumar Debnath, Mr. Kwenga Ismael Munene, Mr. Md. Manowarul Islam, and Mr. Rahardhita Widyatra Sudibyo. I am heartily thankful to all the members of FUNABIKI Lab for their supports during the period of this study. Especially, I wholeheartedly appreciate Dr. Khin Khin Zaw and Mr. Chihiro Taniguchi for their great helps in this study.

Finally, I am eternally grateful to my beloved parents, who always encourage and support me throughout my life. Your supports and understanding gave me the strength and inspiration to overcome any difficulty in my life.

List of Publications

Journal Paper

1. **K. S. Lwin**, N. Funabiki, C. Taniguchi, K. K. Zaw, M. S. A. Mamun, M. Kuribayashi, and W.-C. Kao, "A minimax approach for access point setup optimization in IEEE 802.11n wireless networks," Int. J. Netw. Comput., vol. 7, no. 2, pp. 187-207, July 2017.

International Conference Papers

2. N. Funabiki, C. Taniguchi, **K. S. Lwin**, K. K. Zaw, and W.-C. Kao, "A parameter optimization tool and its application to throughput estimation model for wireless LAN," Proc. Int. Work. Virtual Environ. Netw.-Orient. Appli., Torino, Italy, pp. 701-710, July 2017.

3. **K. S. Lwin**, N. Funabiki, K. K. Zaw, M. S. A. Mamun, and M. Kuribayashi, "A minimax approach for access-point setup optimization using throughput measurements in IEEE 802.11n wireless networks," Proc. Int. Symp. Comput. Networking, Hiroshima, Japan, pp. 311-317, Nov. 2016.

4. N. Funabiki, **K. S. Lwin**, M. Kuribayashi, and I. W. Lai, "Throughput measurements for access-point installation optimization in IEEE 802.11n wireless networks," Proc. IEEE Int. Conf. Consum. Elect. Taiwan, Nantou, Taiwan, pp. 218-219, May 2016.

Other Papers

5. **K. S. Lwin**, N. Funabiki, S. K. Debnath, and M. K. Ismael, "A minimax approach for access-point setup optimization in IEEE 802.11n WLAN with MIMO links," Proc. IEEE Hiroshima Section Student Symp., pp. 234-237, Dec. 2017.

6. **K. S. Lwin**, K. K. Zaw, and N. Funabiki, "Throughput measurement minimization for parameter optimization of throughput estimation model," Proc. Chugoku-Branchi J. Conf., Oct. 2017.

7. **K. S. Lwin**, N. Funabiki, K. K. Zaw, M. S. Al Mamun, and M. Kuribayashi, "Throughput measurements for access-point setup optimization in IEEE802.11n wireless networks," IEICE Tech. Rep., vol.116, no.146, pp. 27-32, July 2016.

8. **K. S. Lwin**, N. Funabiki, and Md. E. Islam, "Throughput measurements with various indoor AP placement conditions for IEEE802.11n wireless networks," Proc. IEICE General Conf., pp. 80-81, March 2016.

9. **K. S. Lwin**, N. Funabiki, Md. E. Islam, C. C. Chew, and Y. Tani, "Throughput measurements in outdoor environment with different AP placement heights and orientations for IEEE 802.11n wireless networks," Proc. IEEE Hiroshima Section Student Symp., pp. 406-409, Nov. 2015.

List of Figures

List of Tables

Contents

Chapter 1

Introduction

1.1 Background

Nowadays, as a great progress of high-speed and cost-effective Internet access network, IEEE 802.11 *wireless local-area network (WLAN)* has become common in our daily life. In WLAN, a user host, where a personal computer (PC) has been commonly used, connects to the *access point (AP)* without a cable. The AP is a connection hub to the Internet. WLAN has several advantages over wired LAN such as user mobility, ease and speed of deployments, flexibility and cost-effectiveness [1]. As a result, WLAN has been deployed in many places including offices, schools, hotels, airports, and even in trains.

IEEE 802.11n protocol has been applied in many WLANs due to the strengths of higher data rates, wider coverage areas, dual band operations, and backward compatibility. IEEE 802.11n protocol adopts several new technologies to increase the data transmission rate up to $600Mbps$, such as the *multiple-input multiple-output (MIMO)*, the *channel bonding*, and the *frame aggregation*. *MIMO* allows a single radio channel to support multiple data streams by using multiple antennas at the transmitter and the receiver [2]. The *channel bonding* increases the data transmission rate by using adjacent multiple channels together as one channel. The *frame aggregation* also increases the data transmission rate by concatenating several data frames into one to reduce the overhead of the header and the tailor.

In a network field of WLAN, the signal propagation from a transmitter is not uniform in the circumferential and vertical directions. The change of the transmitter setup in terms of the height, the orientation, and the precise coordinate can change the receiving signal strength at the receiver. In WLAN, the setup of each AP can be made by the network operator while the setup of any host can be made by the user. Hence, the network operator should optimize the AP setup to enhance the *receiving signal strength (RSS)* at a host in the field and increase the data transmission rate.

Currently, the *single-input single-output (SISO)* has still been common in hosts. *SISO* has the single antenna where the channel capacity is very limited due to weak multipath effects, fading, and interferences. Thus, the AP setup should be optimized to increase the RSS at hosts with SISO.

MIMO has more chance to receive stronger signal by using multiple antennas at AP and host that SISO. Even if one antenna is receiving a weak signal, it is possible to receive a stronger signal from another antenna. It is know that in MIMO, the antenna configuration, the mutual coupling, and the propagation environment may remarkably impact on the MIMO capacity [3, 4, 5, 6, 7, 8, 9, 10, 11, 12]. Thus, the AP setup should also be optimized to increase the RSS at hosts with MIMO.

In this thesis, each AP is expected to be set up properly in terms of the height, the orientation, and the precise coordinate, so that the host will receive the strongest signal from the AP and

improve the throughput performance. Because the signal propagation is not uniform in WLAN, the best height and direction exists for each AP, such that the RSS at its associated host becomes largest. Actually, the orientation of an AP can be changed along the three axes in Figure 1.1.

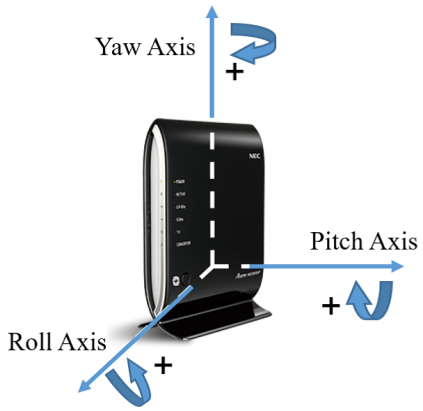

Figure 1.1: Three axes.

In addition, the *multipath effect* can be easily changed to the precise position of the AP. Thus, the precise coordinate to allocate each AP is also important to improve the performance. In this thesis, as this precise position optimization, we consider the coordinate shift of the AP.

1.2 Contributions

In this thesis, we propose the *minimax AP setup optimization approach* to improve the throughput performance of WLAN.

To investigate the significance of the AP setup optimization, we first present throughput measurement results for IEEE 802.11n devices under various placement heights and orientations in outdoor and indoor environments [13, 14, 15]. The commercial devices from three vendors available in Japan, are adopted, namely Buffalo, I-O Data, and NEC. TCP throughput measurements are conducted by changing the height and orientation of the AP with various conditions. The measurement results show that the throughput is greatly affected by the height and orientation of the AP, and confirm the significance of the AP setup optimization.

Next, we propose the *minimax AP setup optimization approach* to improve the throughput performance of WLAN [16, 17, 18, 19]. This approach seeks the maximization of the overall throughput performance of the hosts that are covered by the AP, by finding the AP setup that maximizes the throughput of the host that suffers from the minimum throughput, called *bottleneck host*. In this approach, the bottleneck host is first found by simulations using the *throughput estimation model*. Then, we optimize the AP setup by changing the height, the orientation, and the coordinate of the AP to maximize the throughput of this bottleneck host. Here, we adjust the AP setup condition manually where it is very difficult or impossible to install the machine in the network field due to the cost, the size/weight limitation, and the power supply. To reduce labor loads, the bottleneck host is found by simulations without measuring all host locations.

Third, we propose the *throughput estimation model* to detect a bottleneck host in the network field correctly. This model consists of two steps. In the first step, the *RSS* at the receiver is

estimated using the *log-distance path loss model* [20]. To improve the accuracy in a field with several rooms, the simple model is introduced to consider the *multipath effect*. In the second step, RSS is converted to the throughput using the *sigmoid function*.

Fourth, we propose the *parameter optimization tool* to find the optimal values of the model parameters from the measurement results, based on the algorithm in [21,22]. This tool can be used for various applications, in addition to the throughput estimation model. It seeks the optimal values of the parameters such that the total error between the measured and estimated throughputs is minimized [23]. With using this model, we also propose the *throughput measurement minimization procedure* to minimize the number of throughput measurement points to reduce the labor cost. It selects the limited host locations for throughput measurements to optimize the parameter values while keeping the accuracy [24].

For the evaluations of the proposals, we extensively conducted experiments. First, we measured throughputs for SISO links and MIMO links in the three network fields at two different buildings. Then, we optimized the parameters of the throughput estimation model by using the parameter optimization tool. We evaluated the accuracy of the throughput estimation model with the tool by comparing the measured and estimated throughputs. It was confirmed that the same bottleneck host was found by the model and measurements for any AP location. Finally, we evaluated the minimax AP setup optimization approach through experiments in three network fields using various AP devices from several vendors, and confirmed the effectiveness of this proposal.

1.3 Related Works

Conventionally, APs in WLAN are allocated in the network field after surveying signal strengths of APs at many points using related software tools. In [25], Gibney et al. presented the WLAN modeling, design and evaluation tool that can be used to automatically optimize the number of required APs and the positions to meet site-specific demands in indoor environments. In [26], Lee et al. proposed an approach of optimizing the AP placement and channel assignment in WLANs by formulating the optimal integer linear programming (ILP) problem. To improve the throughput performance, the AP setup optimization could be applied to the APs allocated by these approaches.

Several studies have been reported for antennas and their propagation features in MIMO systems. In [27], Jensen et al. presented that antenna properties such as the radiation pattern, the polarization, the array configuration, and the mutual coupling can impact on MIMO systems. In [28], Zhu et al. introduced a robotic positioning system to automatically control the position and orientation of the antenna array. The results have confirmed that MIMO performance will be notably affected by changing the position and orientation of the antenna array. In [29], Piazza et al. introduced reconfigurable antenna array for MIMO systems. It is proved that different antenna geometry will generate different radiation patterns. In addition, they demonstrated the advantage of changing the antenna configuration based on the spatial characteristics of the MIMO channel. In [30], Forooshani et al. studied the effect of 4×4-ULA (uniform-linear-array) antenna configuration on MIMO-based APs in a real underground service tunnel. It is revealed that the antenna array orientation, the separation, and the polarization will crucially influence the performance of multiple-antenna systems in the underground tunnel.

1.4 Contents of Thesis

The remaining part of this thesis is organized as follows.

In Chapter 2, we introduce wireless network technologies related to this study, such as IEEE 802.11n protocol, the channel bonding, the multiple-input-multiple output (MIMO), antennas in MIMO, and the signal propagation.

In Chapter 3, we provide the throughput measurement results with various heights and orientations of an AP.

In Chapter 4, we propose the minimax AP setup optimization approach.

In Chapter 5, we propose the throughput estimation model.

In Chapter 6, we present the parameter optimization tool for the throughput estimation model.

In Chapter 7, we evaluate the throughput estimation model with the parameter optimization tool in three network fields.

In Chapter 8, we provide the evaluation results for the proposals.

Finally, in Chapter 9, we conclude this thesis and show some future works.

Chapter 2

Background Technologies

In this chapter, we briefly introduce related wireless network technologies as backgrounds for this thesis. First, we overview the *IEEE 802.11 protocol*. Next, we discuss the *IEEE 802.11n protocol* and *IEEE 802.11ac protocol* that are used in our proposal of the minimax AP setup optimization approach. Then, we explain the antenna and radiation pattern in the *MIMO* technology. Finally, we present the effect of the radio propagation onto the signal strength in WLAN.

2.1 Overview of 802.11 WLAN

Wireless local-area network (WLAN) [1] is an alternative or extension to a wired LAN, and supports flexibility for data communications. WLAN can minimize the need for wired connections by transmitting and receiving data over the air using the radio frequency (RF) technology. WLAN can combine the data connectivity with the user mobility.

2.1.1 Advantages of WLAN

WLAN offers the following advantages over a traditional wired LAN [1] due to cable less connections between hosts and hubs:

- *User Mobility:*
  In wired networks, users need to use wired lines to stay connected to the network. On the other hand, WLAN allows user mobility within the coverage area of the network.
- *Easy and rapid deployment:*
  WLAN system can exclude the requirement of network cables between hosts and connection hubs or APs. Thus, the installation of WLAN can be much easier and quicker than wired LAN.
- *Cost:*
  The initial installation cost can be higher than the wired LAN, but the life-cycle costs can be significantly lower. In a dynamic environment requiring frequent movements or reconfigurations of the network, WLAN can provide the long-term cost profit.
- *Increased Flexibility:*
  The network coverage area by WLAN can be easily expanded because the network medium is already everywhere.

- *Scalability:*
  Depending on applications, WLAN can be configured in a variety of topologies. They can support both peer-to-peer networks suitable for a small number of users and full infrastructure networks of thousands of users.

2.1.2 Components of 802.11 WLANs

IEEE 802.11 provides the set of standards for implementing WLAN. IEEE 802.11 WLAN consists of four major physical components as shown in Figure 2.1:

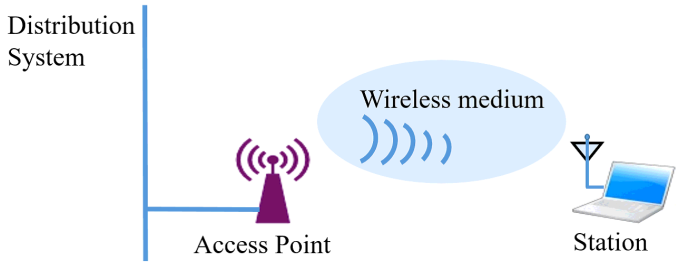

Figure 2.1: Components of 802.11 WLAN.

- *Hosts:*
  WLAN transfers data between *hosts*. A host in WLAN indicates an electronic device such as a desktop/laptop PC, a smartphone, or a Personal Digital Assistants (PDA) that has the capability to access the network over the wireless network interface Card (NIC).

- *Access points (APs):*
  An AP acts as the main radio transceiver or a generic base station for a WLAN that plays the similar role as a hub/switch in wired Ethernet LAN. It also performs the bridging function between the wireless and the wired networks with some other tasks.

- *Wireless medium:*
  The IEEE 802.11 standard uses the wireless medium to flow users information from one host to another host in a network.

- *Distribution system:*
  When several APs are connected together to form a large coverage area, they must communicate with each other to track the movements of the hosts. The distribution system is the logical component of WLAN which serves as the backbone connections among APs. It is often called as the *backbone network* used to relay frames between APs. In most cases, *Ethernet* is commonly used as the backbone network technology.

2.1.3 Types of WLANs

The basic building block of an IEEE 802.11 network is simply a group of stations that communicate with each other called as the *basic service set (BSS)*. BSS can be of two types as illustrated in Figure 2.2.

- *Independent or ad hoc network:* A collection of stations send frames directly to each other. There is no AP in an independent BSS as shown in Figure 2.2(a).
- *Infrastructure network:* The infrastructure network or *infrastructure BSS* uses APs as shown in Figure 2.2(b). When one station communicates with another station, it always communicates through the AP.

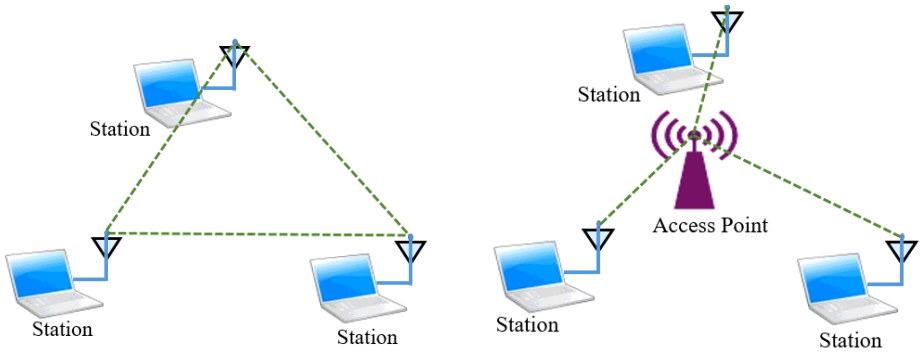

(a) Independent network (b) Infrastructure network

Figure 2.2: Types of 802.11 networks.

- *Extended service area:* Multiple BSSes can be chained together with the same backbone network to form the *extended service set* (ESS) shown in Figure 2.3. It can form large size wireless networks. All the APs in an ESS are given the same *service set identifier* (SSID), which serves as a network "name" for users. Stations within the same ESS can communicate with each other, even if they belong to different basic service areas.

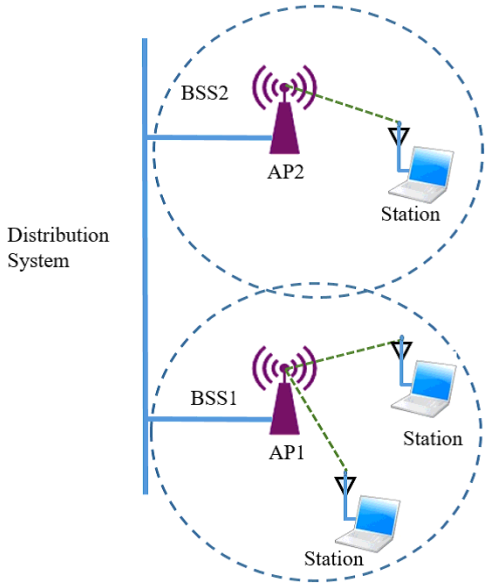

Figure 2.3: Extended service set.

2.1.4 IEEE 802.11 Standards for WLAN

IEEE 802.11 working group enhances the existing *Medium Access Control (MAC)* and *physical layer (PHY)* specification for implementing WLAN in the unlicensed ISM (Industrial, Scientific and Medical) bands defined by the ITU-R (such as 2.4-2.5 GHz , 3.6 GHz and 5.725-5.825 GHz). In this working group, there are several kinds of IEEE Standard Association Standards, which cover from wireless standards, to standards for security aspects, Quality of Service (QoS), and others shown in Table 2.1.4 [31, 32, 33, 34, 35, 36, 37].

Table 2.1: IEEE 802.11 standards.

Standard	**Purpose**
802.11a	Wireless network bearer operating in the 5 GHz ISM band, data rate up to 54 Mbps
802.11b	Operate in the 2.4 GHz ISM band, data rates up to 11 Mbps
802.11c	Covers bridge operation that links to LANs with a similar or identical MAC protocol
802.11d	Support for additional regulatory differences in various countries
802.11e	QoS and prioritization, an enhancement to the 802.11a and 802.11b WLAN specifications
802.11f	Inter-Access Point Protocol for handover, this standard was withdrawn
802.11g	Operate in 2.4 GHz ISM band, data rates up to 54 Mbps
802.11h	Dynamic Frequency Selection (DFS) and Transmit Power Control (TPC)
802.11i	Authentication and encryption
802.11j	Standard of WLAN operation in the 4.9 to 5 GHz band to conform to the Japan's rules
802.11k	Measurement reporting and management of the air interface between several APs
802.11l	Reserved standard, to avoid confusion
802.11m	Provides a unified view of the 802.11 base standard through continuous monitoring, management and maintenance
802.11n	Operate in the 2.4 and 5 GHz ISM bands, data rates up to 600 Mbps
802.11o	Reserved standard, to avoid confusion
802.11p	To provide for wireless access in vehicular environments (WAVE)
802.11r	Fast BSS Transition, supports VoWiFi handoff between access points to enable VoIP roaming on a WiFi network with 802.1X authentication
802.11s	Wireless mesh networking
802.11t	Wireless Performance Prediction (WPP), this standard was cancelled
802.11u	Improvements related to "hotspots" and 3rd party authorization of clients
802.11v	To enable configuring clients while they are connected to the network
802.11w	Protected Management Frames
802.11x	Reserved standard, to avoid confusion
802.11y	Introduction of the new frequency band, 3.65-3.7 GHz in US besides 2.4 and 5 GHz
802.11z	Extensions for Direct Link Setup (DLS)

Table 2.1: IEEE 802.11 standards.

Standard	Purpose
802.11aa	Specifies enhancements to the IEEE 802.11 MAC for robust audio video (AV) streaming
802.11ac	Wireless network bearer operating below 6 GHz to provide data rates of at least 1 Gbps for multi-station operation and 500 Mbps on a single link
802.11ad	Wireless Gigabit Alliance (WiGig), providing very high throughput at frequencies up to 60 GHz
802.11ae	Prioritization of management frames
802.11af	WiFi in TV spectrum white spaces (often called White-Fi)
802.11ah	WiFi uses unlicensed spectrum below 1 GHz, smart metering
802.11ai	Fast initial link setup (FILS)
802.11aj	Operation in the Chinese Milli-Meter Wave (CMMW) frequency bands
802.11ak	General links
802.11aq	Pre-association discovery
802.11ax	High efficiency WLAN, providing 4x the throughput of 802.11ac
802.11ay	Enhancements for Ultra High Throughput in and around the 60 GHz Band
802.11az	Next generation positioning
802.11mc	Maintenance of the IEEE 802.11m standard

Figure 2.4 shows the current and future IEEE 802.11 standards. Among them, 802.11a, 802.11b, 802.11g, 802.11n, and 802.11ac have been popular. For the physical layer, 802.11a/n/ac use *Orthogonal Frequency Division Multiplexing (OFDM)* technology, and 802.11b uses the *Direct Sequence Spread Spectrum (DSSS)* technology. 802.11g supports both technologies. Table 2.2 summarizes features of them [1, 38].

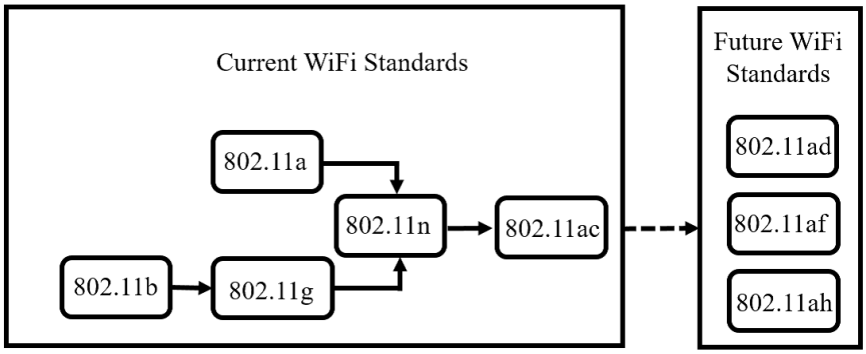

Figure 2.4: Current and future IEEE 802.11 standards.

- *IEEE 802.11b:* The IEEE 802.11b works on the 2.4 GHz frequency band (ISM band) and offers the data rate up to 11 Mbps. The IEEE 802.11b is considered to be a robust system and has a capacity to compensate the same IEEE 802.11 protocols. Because of the interoperability feature between products from different vendors, this standard does not only have boosted the manufacturing of IEEE 802.11b products but also motivated the competition between vendors. The limitation of this standard is the interference among the 802.11b

Table 2.2: Characteristics of common IEEE 802.11 standards.

Standard	802.11b	802.11a	802.11g	802.11n	802.11ac
Release	Sep 1999	Sep 1999	Jun 2003	Oct 2009	Dec 2013
Freq. band	2.4 GHz	5 GHz	2.4 GHz	2.4/5 GHz	5 GHz
Average theoretical speed	11 Mbps	54 Mbps	54 Mbps	600 Mbps	1300 Mbps
Modulation	CCK[1] modulated with PSK	OFDM	DSSS[2], CCK, OFDM	OFDM	OFDM
Channel bandwidth	20 MHz	20 MHz	20 MHz	20/40 MHz	20/40/80/160 MHz
Allowable MIMO streams	1	1	1	4	8
security	Medium	Medium	Medium	High	High

[1] CCK: Complementary Code Keying

[2] DSSS: Direct Sequence Spread Spectrum

products with other products that use *industrial, scientific and medical* (ISM) band that uses the same 2.4 GHz band of frequency [39, 40].

- *IEEE 802.11a:* The IEEE 802.11a operates at the 5 GHz frequency band (*unlicensed national information infrastructure* (UNII) band) and works on OFDM coding scheme that offers a high data rates up to 54 Mbps. Two main limitations of IEEE 802.11a are the compatibility issue of IEEE 802.11a products with IEEE 802.11b products and the unavailability of 5 GHz band with free of costs for all the countries in the world [39, 40].

- *IEEE 802.11g:* IEEE suggested IEEE 802.11g standard over IEEE 802.11a in order to improve the 80211b technology at 2.4 GHz. IEEE 802.11g introduces two different modulation techniques including the *packet binary convolution code (PBCC)* that supports data rate up to 33 Mbps and OFDM that supports up to 54 Mbps data rate. Compatibility issues are also resolved in 802.11g products with 802.11b products [39, 40].

- *IEEE 802.11n:* The main purpose of initiating IEEE 802.11n is to increase the range and improve the data rate up to 600 Mbps. IEEE 802.11n supports both of 2.4 GHz and 5 GHz, and is backward compatible with IEEE 802.11b, 802.11a, and 802.11g. Throughput and coverage range has been improved by introducing new features including use of large bandwidth channels and multiple antennas to get the better reception of RF signals [39, 41].

- *IEEE 802.11ac:* IEEE 802.11ac is aimed at improving the total network throughput as more than 1 Gbps as well as improving the individual link performance. Many of the specifications like static and dynamic channel bondings and simultaneous data streams of IEEE 802.11n have been kept and further enhanced for IEEE 802.11ac to reach the Gigabit transmission rate. It supports static and dynamic channel bondings up to 160 MHz and Multi-user multiple-input multiple-output (MU-MIMO). IEEE 802.11ac operates only on the 5 GHz band [42, 43, 44].

2.2 IEEE 802.11n Protocol

In this section, we overview the IEEE 802.11n protocol that is considered in this thesis. IEEE 802.11n is an amendment to the IEEE 802.11 2007 wireless networking standard. This standard was introduced with 40 MHz bandwidth channels, MIMO, frame aggregation, and security improvements over the previous IEEE 802.11a, 802.11b, and 802.11g protocols. Thus, several researchers have actively studied to evaluate the performance of 802.11n protocol both in indoor and outdoor environments [45, 46, 47].

The IEEE 802.11n is available both on 2.4 GHz and 5 GHz bands. Nowadays, 2.4 GHz is very popular as it was inherited from the IEEE 802.11g. This frequency band has become crowded with lots of WiFi signals using the same channel. As a result, these WiFi signals with adjacent channels will suffer from interferences between them, and end up with throughput performance degrades [36, 37].

For 2.4 GHz band, there is a limited number of non-interfered channels, which are Channel 3 and Channel 11 in 40 MHz bandwidth. While for 20 MHz bandwidth, Channel 1, Channel 6, and Channel 11 are free from interference. In overall, the wider bandwidth will reduce the number of free channels. Figure 2.5 [35] shows the WiFi channels for IEEE 802.11n 2.4 GHz band.

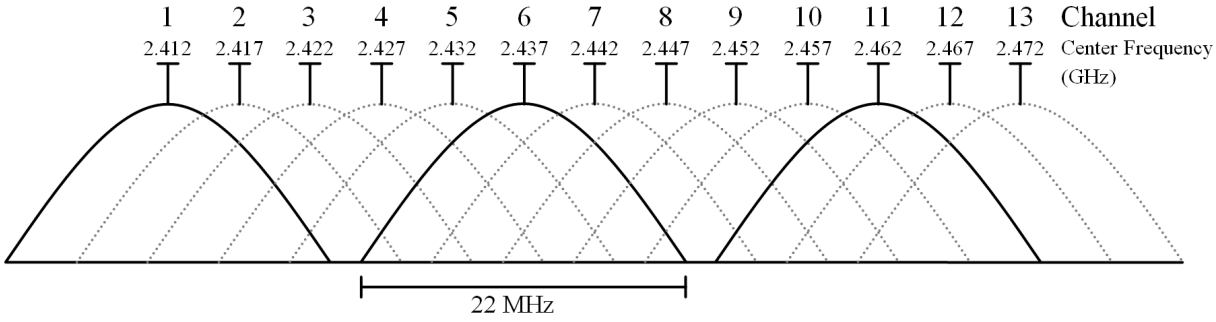

Figure 2.5: WiFi channels in 2.4 GHz band.

For IEEE 802.11n at 5 GHz band, it has a total of 19 uninterrupted channels available in the 20 MHz bandwidth. While in the 40 MHz bandwidth, which doubles the channel width from the 20 MHz, there are 9 channels. For the 80 MHz bandwidth, there are four. Figure 2.6 [48] shows these WiFi channels for the IEEE 802.11n 5 GHz band.

IEEE 802.11n on 2.4 GHz and 5 GHz retain the common 20 MHz channel bandwidth used by the previous 802.11 standards. Through the concept of the channel bonding, whereby two 20 MHz channels are combined into a single 40 MHz channel, the 802.11n had benefited in higher transmission rates [49]. However, the usage of the channel bonding reduces the available channels of WiFi devices as there are only two channels available. Table 2.3 shows the usage of different channel bandwidths and spatial streams towards the throughput of IEEE 802.11n.

In the 802.11n, four spatial streams with up to 150 Mbps/stream are used to reach the maximum data rate (throughput) of 600 Mbps through the MIMO technology. MIMO uses multiple antennas to transmit multiple spatial data streams through *Spatial Division Multiplexing (SDM)*, within one spectral channel of bandwidth. Figure 2.7 shows the comparison between Single Input Single Output (SISO) transmissions and MIMO transmissions. SISO uses one transmitting antenna and one receiving antenna, whereby MIMO uses up to four antennas between devices. The SISO system allowed only one antenna, active during data transmissions, while all antennas in the MIMO system are active simultaneously [2, 50].

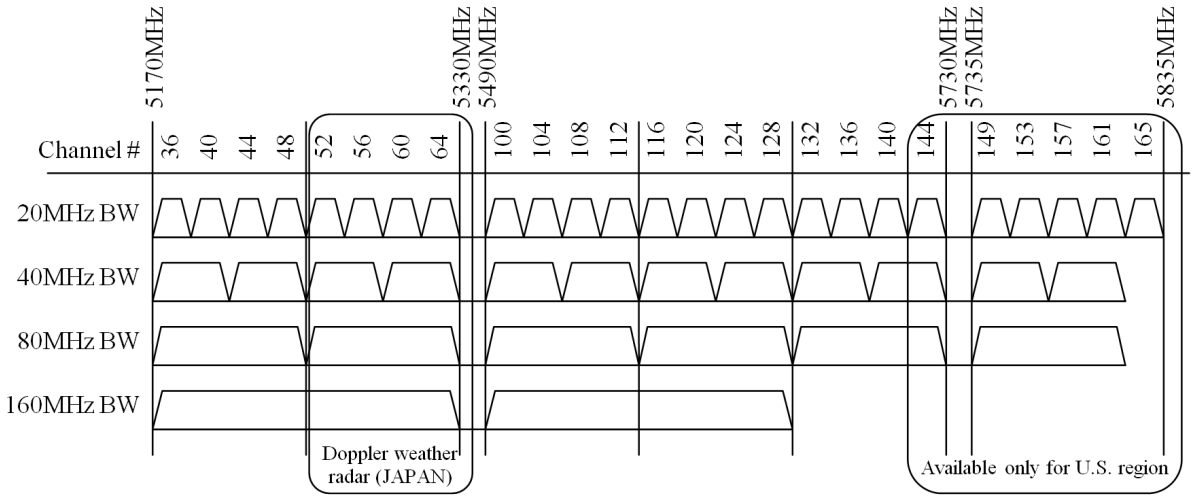

Figure 2.6: WiFi channels in 5 GHz band.

Table 2.3: Effects of channel bandwidth and spatial stream's selection towards IEEE 802.11n's throughput.

Stream number	Bandwidth	
	20 MHz	40 MHz
1 Stream	72.2*Mbps*	150*Mbps*
2 Streams	144.4*Mbps*	300*Mbps*
3 Streams	216.7*Mbps*	450*Mbps*
4 Streams	288.9*Mbps*	600*Mbps*

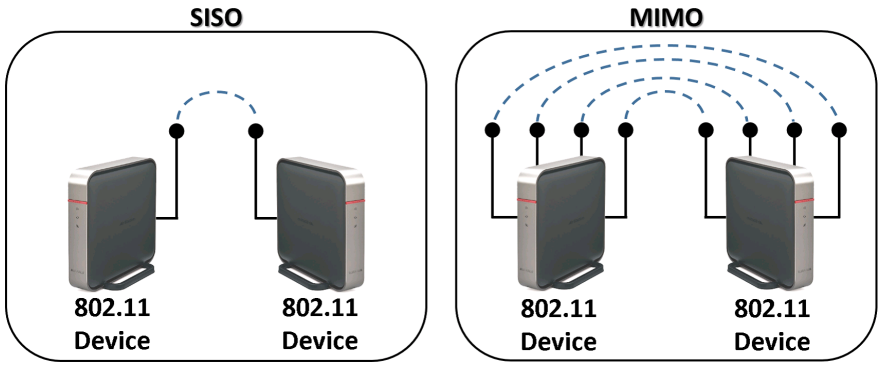

Figure 2.7: Comparison between SISO transmission and MIMO transmission.

Besides the introduction of MIMO, IEEE 802.11n also provides the performance improvement through the frame aggregation in the MAC layer. The frame aggregation can transmit multiple frames by one big frame with a single pre-ample and header information to reduce the overhead by them.

IEEE 802.11n introduces the *Aggregation of MAC Service Data Units (A-MSDUs)* and *Aggregation of MAC Protocol Data Units (A-MPDUs)*. Frame aggregation is a process of packing multiple A-MSDUs and A-MPDUs together to reduce the overheads and average them over multiple frames, thereby increasing the user level data rate [51].

While in the physical layer, IEEE 802.11n use the 64 *Quadrature Amplitude Modulation*

(QAM) scheme under the *Modulation and Coding Scheme (MCS)*. QAM is a form of modulation technique used for modulating digital information signals. QAM exists in both analogue and digital formats. For IEEE 802.11n, the digital QAM format is used and named as Quantized QAM. In QAM, the digital information is encoded in bit sequences represented by discrete amplitude levels of an analog carrier. Two carriers are shifted in phase of 90° with output varies in both amplitude and phase. For 64 QAM, six bits of input alters the phase and amplitude of the carrier to generate 64 modulation states.

2.3 IEEE 802.11ac Protocol

In this section, we overview IEEE 802.11ac protocol. IEEE 802.11ac is an amendment to the IEEE 802.11 2007 wireless networking standard. This standard was introduced with the 5 GHz frequency band, 160 MHz bandwidth channels, MU-MIMO, the increased number of spatial streams, and the higher order of modulations over the previous IEEE 802.11n protocol [36,42,43]. Table 2.4 shows a brief summary about this standard.

Table 2.4: IEEE 802.11ac specification.

Specification	IEEE 802.11ac
Frequency Band	5 GHz
Simultaneous Uninterrupted Channel	9 ch
Available Channel	19 ch
Max Speed	6.93 Gbps
Max Bandwidth	160 MHz
Max Spatial Streams	8
Subcarrier Modulation Scheme	256 QAM
Release Date	Dec 2012

IEEE 802.11ac at 5 GHz band having the same WiFi channels with IEEE 802.11n at 5 GHz, as shown in Figure 2.6. In this frequency band, there are nine non-interfered channels. For 80 MHz bandwidth, which doubles the channel width from 40 MHz, there are four channels, while for 160 MHz bandwidth, there will be two. These channels are same with the 5 GHz IEEE 802.11n, as shown in Figure 2.6.

The channel bonding can increase the data transmission capacity by bonding two or more adjacent channels into one channel. IEEE 802.11ac allows to bond maximally eight 20 MHz channels into one 160 MHz channel. Thus, IEEE 802.11ac can use up to 468 sub-carriers at the 160 MHz channel, whereas the previous IEEE 802.11n does 108 sub-carriers there in the 40 MHz channel [52]. This sub-carrier increase can also enhance the data capacity by more than twice.

It is noted that, within a crowded environment, if multiple IEEE 802.11ac APs are in use, the number of non-overlapping channels will drop down to 9, 4, and 2, using the channel bonding for the bandwidth of 40 MHz, 80 MHz, and 160 MHz respectively. In order to avoid interferences between APs, the lower channel bandwidth will provide fairer performance for all users. Table 2.5 shows the usage of different channel bandwidths and spatial streams towards the throughput of IEEE 802.11ac.

In IEEE 802.11ac, eight spatial streams can be used to transmit up to 866.7 Mbps/stream and reach the maximum data rate (throughput) of 6,933 Mbps through the MIMO technology. MIMO

Table 2.5: Effects of channel bandwidth and spatial stream's selection towards IEEE 802.11ac's throughput.

Stream Number	Bandwidth			
	20 MHz	40 MHz	80 MHz	160 MHz
1 Stream	86.7*Mbps*	200*Mbps*	433.3*Mbps*	866.7*Mbps*
2 Streams	173.3*Mbps*	400*Mbps*	866.7*Mbps*	1733*Mbps*
3 Streams	288.9*Mbps*	600*Mbps*	1300*Mbps*	2340*Mbps*
4 Streams	346.7*Mbps*	800*Mbps*	1733*Mbps*	3466*Mbps*
8 Streams	693.4*Mbps*	1600*Mbps*	3466*Mbps*	6933*Mbps*

can transmit multiple data in parallel by adopting multiple antennas. For example, when the source node and the destination node have two antennas respectively, the transmission speed becomes doubled using two data streams. IEEE 802.11ac allows the maximum of eight antennas.

Besides that, IEEE 802.11ac also comes with the MU-MIMO, which allows an AP to transmit data to multiple hosts in a parallel way without interferences between them by adopting the beamforming technology that generates directional radio signals. This is far faster than the serial communication in IEEE 802.11n. MU-MIMO can realize 1-to-n data transmissions using the same band. Figure 2.8 compares the single-user MIMO technologies used in 802.11n with the new multi-user MIMO in 802.11ac [44].

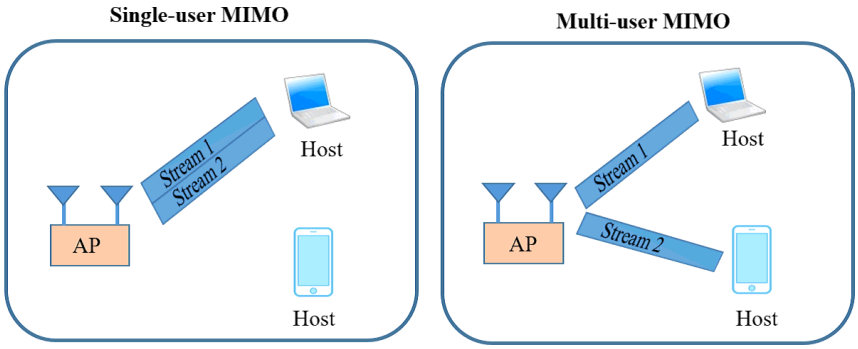

Figure 2.8: Multi-user MIMO comparison.

Apart from the MU-MIMO, IEEE 802.11ac also introduces the beamforming technology. In beamforming, a sender detects where the receiver are and transmits data through intensifying the signal in their direction(s). The focus of radio frequency energy towards the receiver will provide the higher signal strength to increase the speed. This is better than the traditional way of broadcasting wireless signals equally in omni directions. Figure 2.9 shows the different between the usage of beamforming technology and normal WiFi.

The IEEE 802.11ac also inherits the A-MSDU and A-MPDU from IEEE 802.11n, and allows the maximum of 1 Mbyte for one frame, whereas IEEE 802.11n does 64 Kbyte.

In order to gain the higher transmission rate, the *Guard Interval (GI)* that represents the period between two consecutive packet transmissions also has been reduced. GI is necessary to avoid interferences between them that can be caused by the delay of the first packet arrives at the destination node. IEEE 802.11ac adopts 400 ns as the guard interval time, whereas 11a/g does 800 ns.

In the physical layer, IEEE 802.11ac use the 256 QAM scheme under the MCS. In 256 QAM,

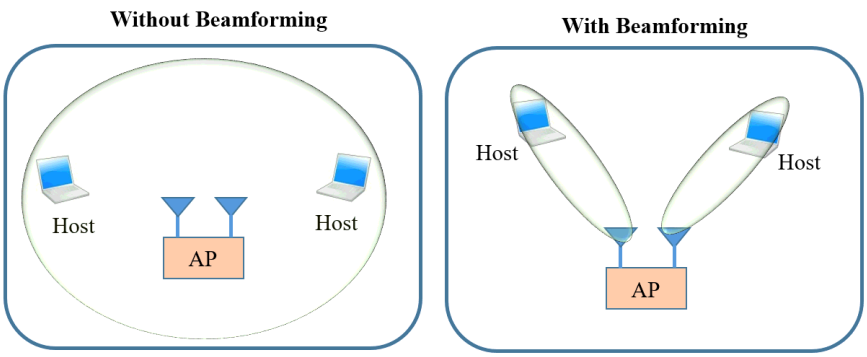

Figure 2.9: Beamforming technology.

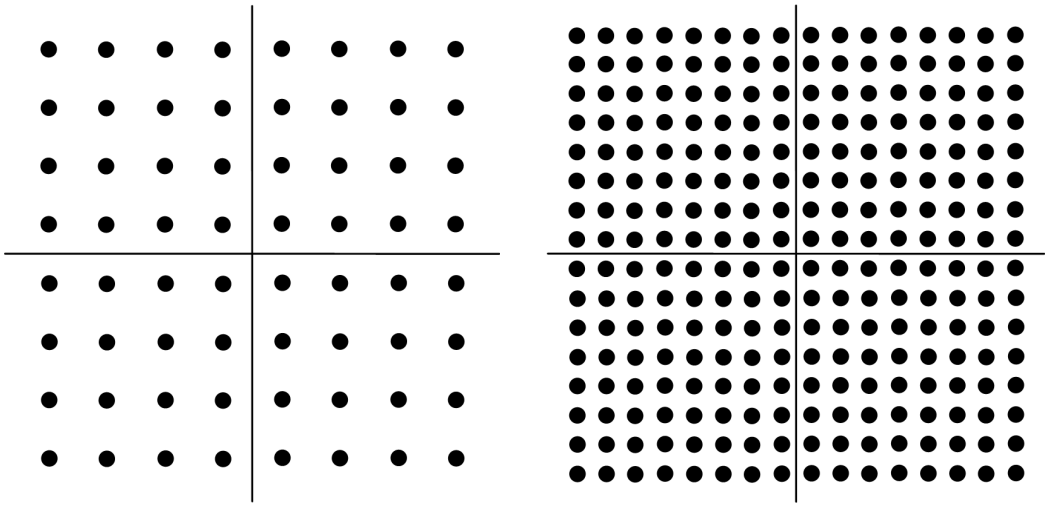

(a) 64 QAM (b) 256 QAM

Figure 2.10: Comparison of modulation.

eight bits of input alters the phase and amplitude of the carrier to generate 256 modulation states. Figure 2.10 shows the comparison between 64 QAM constellation (IEEE 802.11n) to the 256 QAM constellation.

2.4 Multiple Antennas in MIMO

IEEE 802.11n and 802.11ac protocols adopt MIMO to increase the transmission capacity. MIMO not only takes the advantage of multipath communications using multiple antennas at the transmitter and the receiver, but also enhances the performance of the wireless communication system. Due to the increasing computing power of the embedded CPU and the reducing device size, multiple antennas and complex signal processing programs could be implemented on one board. Figure 2.11 demonstrates the internal antenna layout of NEC WG2600HP AP [53] with four antennas for MIMO.

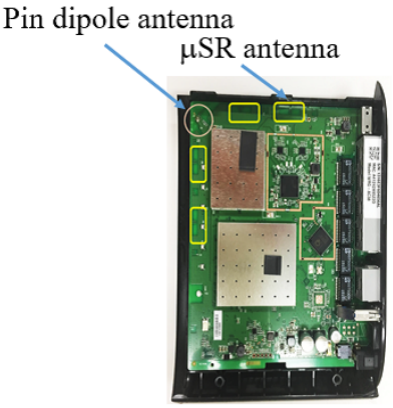

Figure 2.11: Internal antenna layout of NEC WG2600HP.

2.5 Non-symmetric Radiations in MIMO

The multiple antenna layout of the MIMO device will make a significant impact on the overall radiation pattern and strongly affect the performance of the device [29, 54, 55]. In general, an antenna could be categorized as the *omnidirectional antenna* and the *directional antenna* based on the radiation pattern. Most of APs and mobile devices deploy the omnidirectional antenna, either monopole or dipole. Figure 2.12 exhibits the radiation patterns of two dipole antennas that are separated by 0.25λ at the operating frequency of 2.45 GHz for the MIMO system [29].

Due to the multiple antennas, the radiation pattern of the MIMO device is not symmetric in the horizontal and vertical directions, as shown in Figure 2.12 (a) and (b) respectively. Particularly, for the vertically polarized omnidirectional antenna, it radiates the strongest signal power in the horizontal direction, dropping to zero directly above and below the antenna [56].

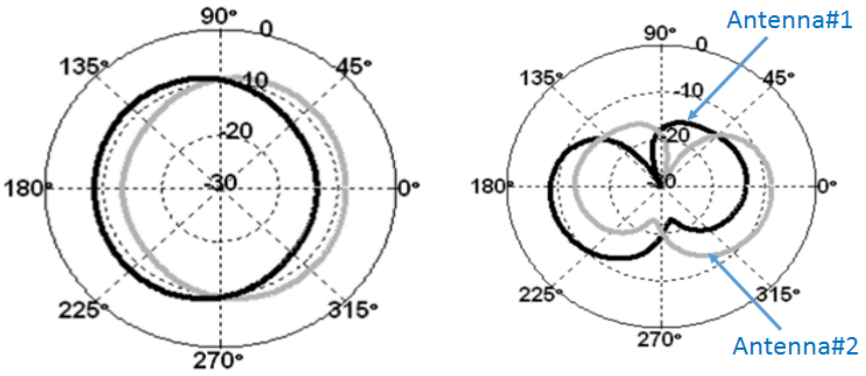

(a) E Plane (b) H Plane

Figure 2.12: Radiation pattern (in dB) of two antennas at 2.4 GHz.

2.6 Signal Propagation in WLAN

Since a WLAN system is based on radio frequency (RF) signals, the communication quality depends on the signal strength between transmitter and receiver. In a real network field, the signal strength can be affected by various propagation mechanisms including reflection, diffractions, refraction, scattering, and absorption [57]. Generally, these effects can be varied by the surrounding environments and the frequency of the signal used. Thus, the signal strength, range and coverage area of an AP is strongly affected by its position, placement and installation environments [58]. For MIMO devices, the propagation of the radio signals become more complex due to the multiple antennas adopted at transmitter and receiver.

Besides, the RF signal at 2.4 GHz and 5 GHz become weak after penetrating obstacles such as concrete walls in a building, then the link speed or throughput become low. For indoor environments, depending on the material and thickness, the walls and obstacles can make the signal loss. This signal loss or attenuation factor should be taken into considerations for WLAN design. Table 2.6 shows the approximate losses for different building materials at 2.4 GHz [59].

Table 2.6: Typical attenuation for building materials at 2.4 GHz.

Range	Materials	Loss (dB)
Low	Non tinted glass, Wooden doors, Cinder block walls, Plaster	2-4
Medium	Brick wall, Marbl, Wire mesh, Metal tinted glass	5-8
High	Concrete wall, Paper, Ceramic bullet-proof glass	10-15
Very high	Metals, Silvering (Mirrors)	>15

2.7 Summary

In this chapter, we introduced related wireless network technologies, including IEEE 802.11n and 802.11ac protocols, to this thesis. Then, we described the multiple antenna layout of a commercial AP and the radiation pattern in MIMO that can affect the performance of WLAN. After that, we discussed the signal propagation and attenuation factors in WLAN. In the next chapter, we will explore the effect of AP setup conditions on throughput performance by adopting commercial MIMO APs in real network fields.

Chapter 3

Throughput Measurements with Various Heights and Orientations of Access-Point

In this chapter, we present extensive throughput measurement results using *transmission control protocol (TCP)* under various conditions in outdoor and indoor environments, to investigate the significance of the *access-point (AP)* setup optimization. TCP has been used in major Internet applications such as the World-Wide Web, the email, the remote administration, and the file transfer protocol (FTP).

3.1 Measurement Setup

In the measurements, we adopt one commercial AP (Buffalo WZR-1750DHP) [60] and two laptop PCs with Windows OS. One PC is used for the server that is connected with the AP through JMicro JMC250 Gigabit Ethernet adapter. Another PC is used for the client that is connected with the AP through Qualcomm Atheros AR9285 IEEE802.11b/g/n wireless adapter. Figure 3.1 shows the network configuration in the measurements.

Before measurements, we disabled the unnecessary programs to maintain the high performance of PCs, and run *SG TCP optimizer software* [61] to optimize the network adapters, where the *maximum transmission unit (MTU)* value was set to 1500 bytes [39]. Then, we used *Wi-Fi Channel Scanner* [62] to check the frequency band activity in 2.4 GHz in the field. From this result, the 40 MHz bounded channel 9 + 13 was used for measurements as the lowest wireless interference. By using *iperf* [63], TCP traffics are generated in both directions for 50 seconds. The TCP window size and the buffer size were set 477 Kbytes and 8 Kbyte respectively.

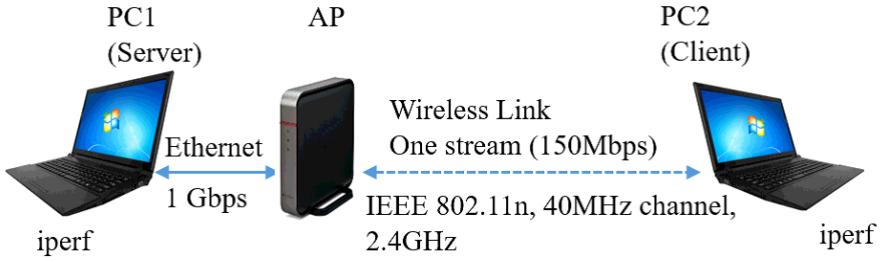

Figure 3.1: Measurement network topology.

3.2 Outdoor Environment

As the outdoor environment, throughput measurements were conducted near the Faculty of Agriculture in the Okayama University campus. This place has less interfered wireless signals and human activities. Figure 3.2 shows the field photo in our measurements. One-story building is located on the right side, and several trees are on the left side. According to Japan Meteorological Agency [64], the temperature was around 29°C and the relative humidity was around 77% that can be necessary to consider thermal fade interference [36].

Figure 3.2: Experiment field for measurements.

3.3 Measurement Scenarios

While the throughput measurements, the *device placement height* and the *AP orientation* are changed. To change the height, two plastic shelves with five levels were used where one level height is 0.45m. Thus, we could change the height up to 1.80m with 0.45m increment. The distance between AP and PC2 was fixed at 40m in the direct line-of-sight (LOS), and AP was placed -30° angle to the left side from the center by [65].

For *different placement heights*, the following three scenarios were considered:

1. Scenario 1: change the height of both AP and PC2 to 0.00m, 0.45m, 0.90m, 1.35m, and 1.80m simultaneously.

2. Scenario 2: change only the height of PC2 to 0.00m, 0.45m, 0.90m, 1.35m, and 1.80m while fixing the height of AP at the proper one according to the results of *Scenario 1*.

3. Scenario 3: change the height of only AP to 0.00m, 0.45m, 0.90m, 1.35m, and 1.80m while fixing the height of PC2 at the proper one according to the results of *Scenario 1*.

For *different placement orientations*, the placement heights of AP and PC2 were fixed based on the results for different placement heights. Then, the throughput was measured while changing

the orientation of AP one by one, on the roll axis, the yaw axis, and the pitch axis, shown in Figure 3.12. As the angles to be measured, we used 0°, ±30°, ±60°, and ±90° of all axes.

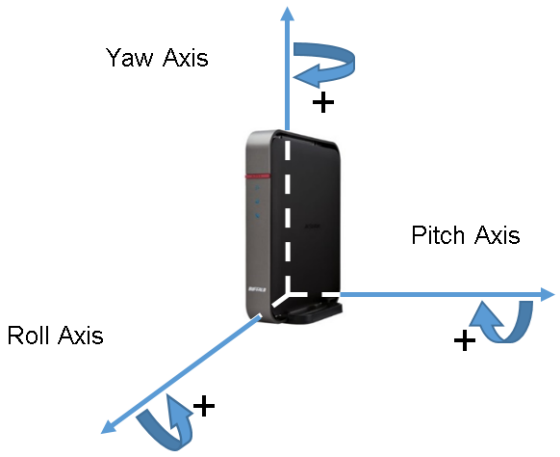

Figure 3.3: AP orientations for measurements.

3.4 Results in Outdoor Environment

In this section, we present the throughput measurement results that are affected by *different placement heights* and *different placement orientations* of the devices.

3.4.1 Results for Different Heights

First, we show the results for *different placement heights* with three scenarios. Figure 3.4 (a) shows the results for *Scenario 1*. The throughput becomes peak when the height is 0.90m in either direction. We suppose that the multipath effect by reflections at the ground affects this result.

Then, Figure 3.4 (b) shows the results for *Scenario 2*, when the height of AP is fixed to 0.90m. The throughput becomes peak when the height of PC2 is 1.35m in either direction.

Finally, Figure 3.4 (c) shows the results for *Scenario 3*, when the height of PC2 is fixed to 0.90m. The throughput becomes peak when the height of AP is 0.9m in the downlink and 1.35m in the uplink.

From these results, we can observe that 1) the throughput becomes highest at 0.9m and lowest at 0.00m height, and 2) the downlink throughput is higher than the uplink one because the transmission power and the antenna size of AP are larger than PC.

Our measurement results for *different placement heights* indicate the importance of the proper height in the AP placement for the best throughput.

3.4.2 Results for Different Orientations

The measurements for *different placement orientations* were carried out only for downlink transmissions from the server to the host, to figure out the effect of the AP orientations change to the receiving signal strength change at the host. The heights of AP and PC2 were fixed at 0.90m and 1.35m respectively. Then, we changed the angles of AP on the axes in roll, yaw, and pitch one by one while the PC2 was fixed in normal.

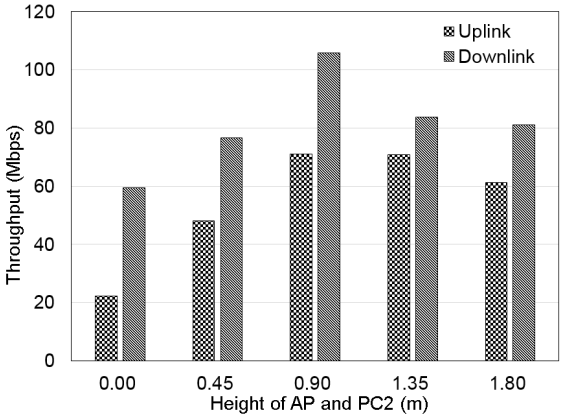

(a) Same heights of AP and PC2

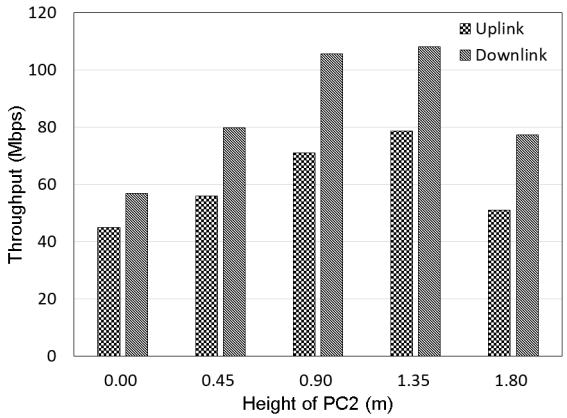

(b) Different heights of PC2

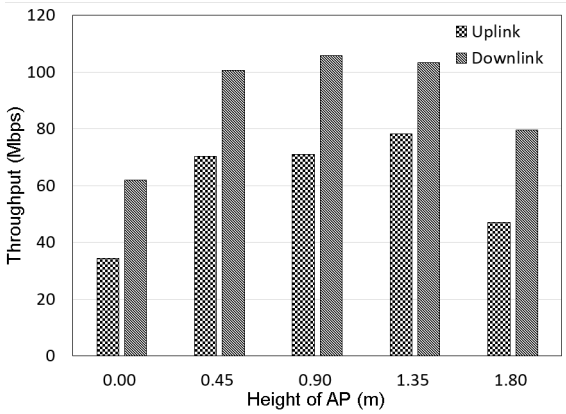

(c) Different heights of AP

Figure 3.4: Throughput results for different heights.

First, we changed the angle on the yaw axis from -90° to +90° while the angles on the other axes were fixed at 0 °. Figure 3.5 (a) shows the results, where the throughputs at -30°, -60°, -90 °, and +90° are better than other angles. We suppose that the multipath effect by reflections from the one-story building at the left side affects these results.

Then, we changed the angle on the roll axis from -90° to +90° while the angles on the other axes were fixed at 0°. Figure 3.5 (b) shows the results, where the throughput becomes peak at -30°. This might be internal omnidirectional antennas of AP used in our measurements because the coverage of the antennas can be changed by varying the angles of antennas.

Finally, we changed the angle on the pitch axis from -90° to +90° while the angles on the other axes were fixed at 0°. Figure 3.5 (c) shows the results, where the throughput becomes maximum except at 0°. We suppose that these results also depend on the orientation of internal antennas of AP that has four antennas on the top side and two in the front side. Our measurement results for *different placement orientations* show that the throughput can be optimized by changing the orientations of AP. It is also node that the environments and orientations of the internal antennas should be taken into consideration for improving the throughput. In summary, the results indicate the importance of the proper orientation in the AP placement for the best throughput.

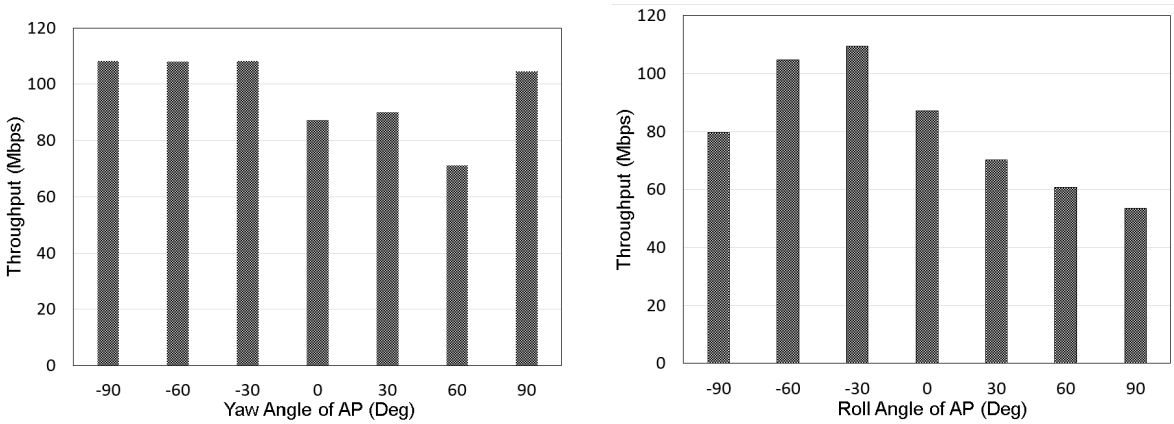

(a) Yaw angles of AP

(b) Roll angles of AP

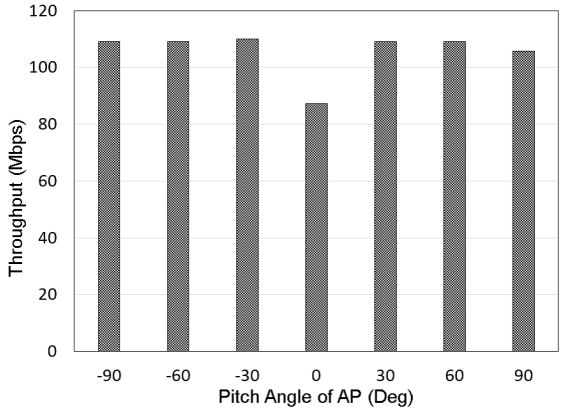

(c) Pitch angles of AP

Figure 3.5: Throughput results for different orientations.

3.5 Indoor Environment

Next, we performed the measurements in Engineering Building#2 of Okayama University campus. Here, we can observe many Wi-Fi signals. We used APs from three different vendors: NEC WG2600HP [53], Buffalo WZR-17500HP [60], and I-O Data WN-AC1600DGR [66] in Figure 3.6. Figure 3.7 shows the locations of the AP and the client PC where at least one concrete wall exists between them in the non-line-of-sight (NLOS).

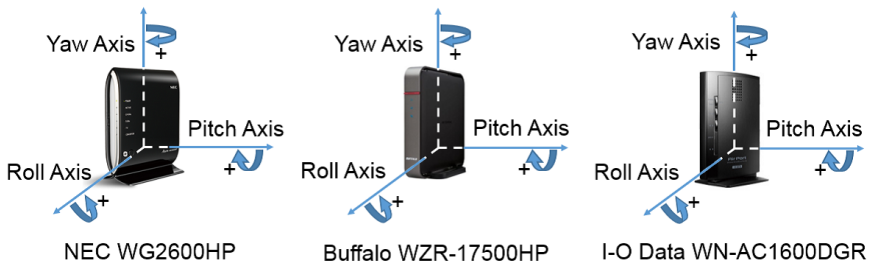

Figure 3.6: APs from three different vendors.

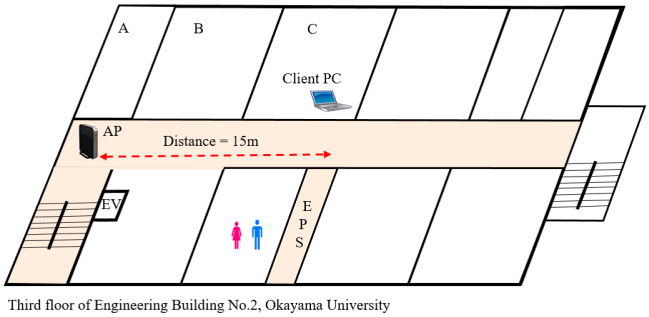

Figure 3.7: Device locations for measurements.

3.6 Results in Indoor Environment

We conducted the throughput measurements by changing the height and the orientation of AP. In the measurements, the height of the client PC was fixed at with 0.45m, and the back side of the screen of the PC was facing to the AP. Throughput measurements followed the AP setup in Section 3.1 for the indoor environment.

3.6.1 Results for Different Heights

First, we changed the height of AP up to 1.80m with 0.45m increment while the orientation angles on the three axes were fixed at 0°. Figure 3.8 shows the measurement results. The throughput at 1.35m height provides the best for all the APs. Generally, the throughputs by IO-Data are higher than the others by changing the height of AP.

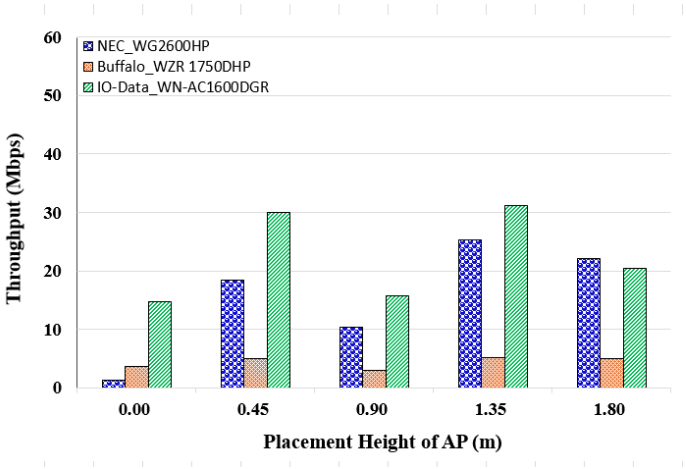

Figure 3.8: Throughput results for different height of AP.

3.6.2 Results for Different Roll Angles

Next, we changed the angle on the roll axis from -90° to +90° while we fixed the angles on the other axes at 0° and the best height at 1.35m. Figure 3.5c shows the measurement results. The

throughput at +90°, which indicates to lay down the AP, is the best for NEC and Buffalo, and that at -30° is the best for IO-Data. Generally, the throughputs by NEC are higher than the others.

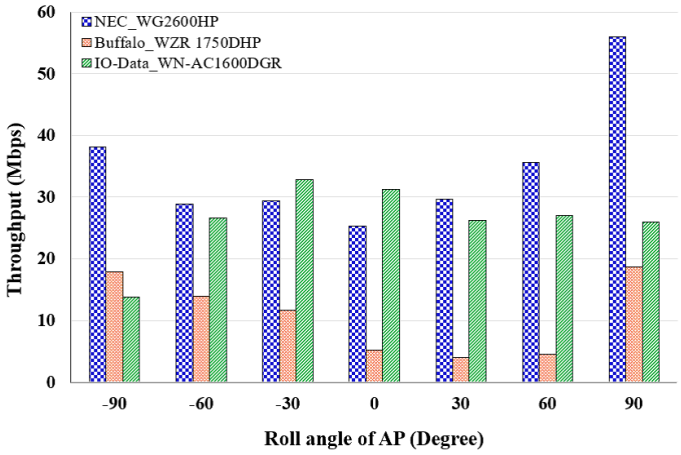

Figure 3.9: Throughput results for different roll angles of AP.

3.6.3 Results for Different Yaw Angles

Then, we changed the angle on the yaw axis from 90° to +90° while we fixed the angles on the other axes at 0° and the best height at 1.35m. Figure 3.10 shows the measurement results. The throughput at 30° is the best for NEC and IO-Data, and the one at -60° is the best for Buffalo. The throughput by IO-Data is more stable and is generally higher than the others.

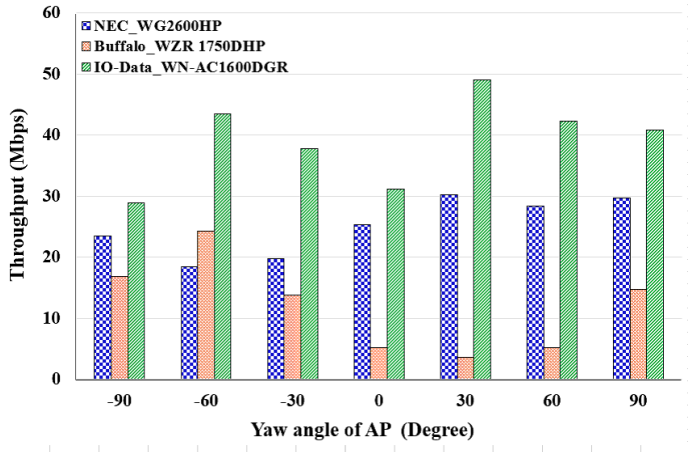

Figure 3.10: Throughput results for different yaw angles of AP.

3.6.4 Results for Orientation Optimization

Finally, to further improve the throughput, we changed both the roll and yaw angles at the same time. Figure 3.11 shows the measurement results. For example, NEC_R+90_Y+30 indicates that we changed the roll angle at 90° and the yaw angle at 30° simultaneously. The results show that the throughput at NEC_R+90_Y+0 is the best among them. The one at IO-Data_R0_Y+30 is the second best and the one at Buffalo_R+90_Y-60 is the last.

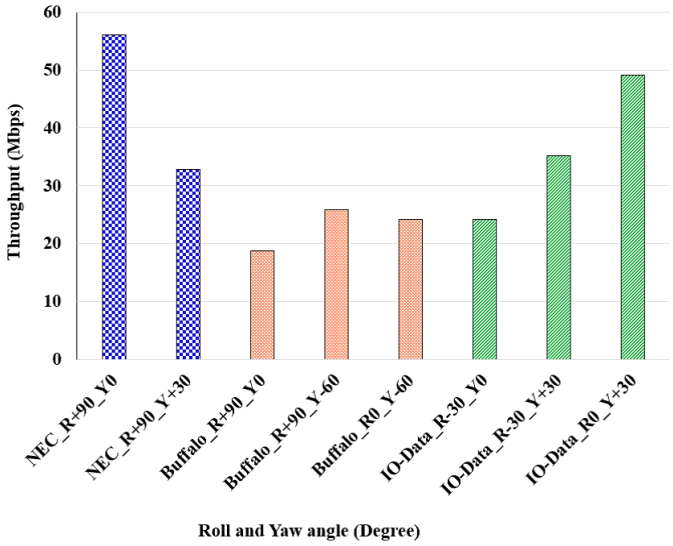

Figure 3.11: Throughput results for angle optimization.

3.6.5 Observation

Our measurement results show that the throughput performance is strongly affected by the roll and yaw angles of AP. It may come from the structure of the internal antennas in each device and signal propagations in the network field. In the measurement setup, the transmission signal can be reflected at the floor or the ceiling strongly due to the indoor environment. It can lead to the best throughput at the laid down of AP.

For reference, Figure 3.12 shows the internal structure of the Buffalo AP. We can observe three antennas for transmitters and receivers on the same plane. Thus, when they are faced to the direction of coming strong signals, the throughput becomes highest. However, the best roll/yaw angles generally depend on the field and the device architecture.

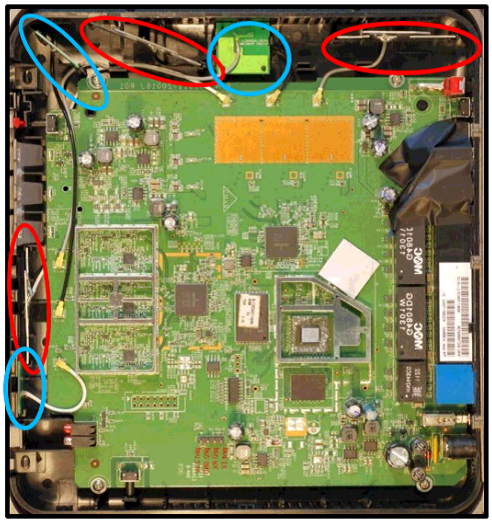

Figure 3.12: MIMO antennas in Buffalo AP.

3.7 Summary

In this chapter, we presented TCP throughput measurement results for IEEE 802.11n commercial APs and PCs under various placement heights and orientations in outdoor and indoor environments. We also provided throughput measurement results for three APs from different vendors in the indoor environment. Our results show that the throughput of the IEEE 802.11n link can be strongly affected by the placement height and the roll angles of AP.

Chapter 4

Proposal of Minimax Access-Point Setup Optimization Approach

In this section, we present the *minimax access-point setup optimization approach* in WLAN.

4.1 Overview

As mentioned in the previous section, the setup of the IEEE 802.11n AP has essential effects on the performance of WLAN. To optimize the AP setup while reducing the labor cost, we propose the *minimax AP setup optimization approach*. In this approach, the manual setup adjustments of the AP are merely applied for the maximization of the throughput between the AP and the bottleneck host in the network field. This *bottleneck host* is found through simulations using the *throughput estimation model*. To improve the estimation accuracy, the parameters in the model is tuned using the *parameter optimization tool* with the throughput measurement results for the hosts in the network field.

4.2 AP Setup Optimization Steps

The proposed approach consists of the following five steps:

(1) The layout map of the target network field for WLAN is obtained, and the possible locations of the APs and the hosts are identified on the map.

(2) The throughputs between the APs and the hosts in (1) are measured.

(3) The parameters of the throughput estimation model are tuned by applying the parameter optimization tool with the measured data in (2).

(4) The bottleneck host for each AP is detected using the throughput estimation model. Here, it is assumed that if a host can be associated with multiple APs in the field, it will be associated with the AP that provides the highest throughput among them in the model.

(5) The setup of each AP is manually adjusted such that the measured throughput to the corresponding bottleneck host is maximized.

4.3 Justification of Minimax Approach

The motivation of this minimax approach is to minimize the labor cost for optimizing the AP setup in terms of the height, the orientation, and the coordinate. Currently, it is not considered to optimize the AP setup automatically or remotely using a machine that can adjust the AP setup, because of the cost. Moreover, it is exceedingly difficult or impossible to install the machine in the network field due to the size/weight limitation and the power supply at the AP installation point. Thus, we consider the manual setup of the AP as the only way to achieve the goal, where we have to minimize the labor cost for this setup optimization. In this thesis, it is clarified that the optimal setup of an AP for the bottleneck host will improve the overall throughput for the hosts in the network field that are covered by the same AP.

Chapter 5

Proposal of Throughput Estimation Model

In this chapter, we present the throughput estimation model for the proposed minimax AP setup optimization approach.

5.1 Introducton

In the minimax AP setup optimization approach presented in Chapter 4, the bottleneck host is first found through simulations using the *throughput estimation model* to reduce the labor cost. Then, the AP setup is optimized by changing the height, the orientation, and the coordinate of the AP so that the throughput of this bottleneck host is maximized.

In this chapter, we present the *throughput estimation model* to accurately estimate the throughput or transmission speed of a wireless communication link between a source node and a destination node in WLAN. First, this model estimates the *receiving signal strength (RSS)* at the destination node using the *log-distance path loss model* that considers the distance and the obstacles between the nodes. Next, it estimates the throughput from the RSS using the *sigmoid function*. Each function possesses several parameters whose values affect the estimation accuracy.

In the two functions of the model, the specifications of a wireless link, such as the adopted protocol, the number of streams for MIMO, the use of the channel bonding and the frame aggregation, should be considered in the parameter values. In our measurements, we used one stream for SISO links and two streams for MIMO links, the channel bonding, and the frame aggregation. To obtain the parameter values of the model for other specifications such as three or more streams, the measurements using the corresponding AP configurations will be necessary, which will be included in future studies.

5.2 Related Works

A variety of studies have been addressed to the issue of the propagation signal prediction in WLAN.

In [67], Wolfe et al. proposed a dominant path prediction model for indoor scenarios. Several factors such as the path length, the number, and the type of interactions, the material properties of obstacles along the path are considered for the prediction of the path loss between the transmitter and the receiver.

In [68], Plets et al. proposed an algorithm for the indoor path loss prediction at 2.4 GHz. The authors performed the measurements on one floor of an office building to investigate propagation characteristics. They presented the path loss model by considering the distance loss, the cumulated

wall loss, and the interaction loss. The accuracy of this prediction is verified with measurements in four buildings.

In [69], Dama et al. presented a signal strength prediction of a field with $1728m^2$ area with 2.4GHz and 5GHz by implementing a simulated propagation model using 3D Shoot and Bounce Ray (SBR) software. The accuracy of the model is confirmed by the measurement results using a commercial wireless router with 2×3 dual-band MIMO system in the corridor. They did not consider the building layout such as walls and material properties.

These works did not consider the throughput estimation and the parameter optimization for WLAN. Our model can be applied to realistic office environments and be used in the *WIMNET simulator* [70]. It can simulate a complex floor layout of multiple rooms that may have different sizes and shapes, which are not supported in the NS3 simulator [71].

5.3 Signal Strength Estimation by Log-distance Path Loss Model

The RSS of a host from the AP is estimated using the *log-distance path loss model* [20]:

$$P_d = P_1 - 10\alpha \log_{10} d - \sum_k n_k W_k \tag{5.1}$$

where P_d represents the RSS (dBm) at the host, d does the distance (m) to the host from the AP, P_1 does the RSS (dBm) at the host at the $1m$ distance from the AP when no obstacle exists between them, α does the path loss exponent, n_k does the number of *type k* obstacles along the path between the AP and the host, and W_k does the signal attenuation factor (dB) for the *type k* obstacle. The value for α strongly depends on the network environment. In [20], the proper value for α has empirically been determined between 1.8 (lightly obstructed environment with corridors) and 5 (multi-floored buildings).

For the signal attenuation factor W_k of walls, the six types of obstacles are considered in this thesis. They include the corridor wall, the partition wall, the intervening wall, the glass wall, the elevator wall, and the door. The *corridor wall* represents the concrete wall between a room and the corridor that has the sufficient strength to improve the strength of the building itself. The *partition wall* indicates the wall without the sufficient strength and simply separates the successive rooms. The *intervening wall* signifies the concrete wall that has the sufficient strength, but does not separate closed rooms. The *glass wall* implies the wall composed of glass panels mounted in aluminum frames. The *elevator wall* represents the steel wall of the elevator. The *door* represents the entering door of the room with a glass, where its open/close can affect the signal propagation in the room [72].

It is noted that α can be replaced by α_{inc} (the enhanced path loss exponent factor) if $d \geq d_{thr}$ (the distance threshold) to improve the estimation accuracy, because the prediction accuracy can become poor at longer distances from the transmitter [73, 74, 75].

5.4 Throughput Estimation from Received Signal Strength

From the RSS at the host, the throughput or data transmission speed of a link between the AP and the host is calculated using the *sigmoid function*:

$$S = \frac{a}{1 + \exp\left(-\frac{(120+P_d)-b}{c}\right)} \tag{5.2}$$

where S represents the estimated throughput (Mbps) when the RSS (dBm) at the host is P_d. a, b, and c are parameters to be tuned.

The adoption of the sigmoid function for the throughput estimation is based on our measurement results. Figure 5.1 reveals the relationship between signal strengths and throughputs for the SISO link. The data were collected through experiments using NEC WG2600HP [15] for the AP, two Windows PCs with JMicro JMC250 Gigabit Ethernet adapter and Qualcomm Atheros AR9285 IEEE 802.11b/g/n wireless adapter for the server and the host, *iperf* for the throughput measurement software [63], and *Homedale* [76] for the receiving signal strength measurement software. They were conducted in an indoor environment at Okayama University. The sigmoid function curve was illustrated there using $a = 98$, $b = 55$ and $c = 8$. The curve is well coincident with the measured data [77].

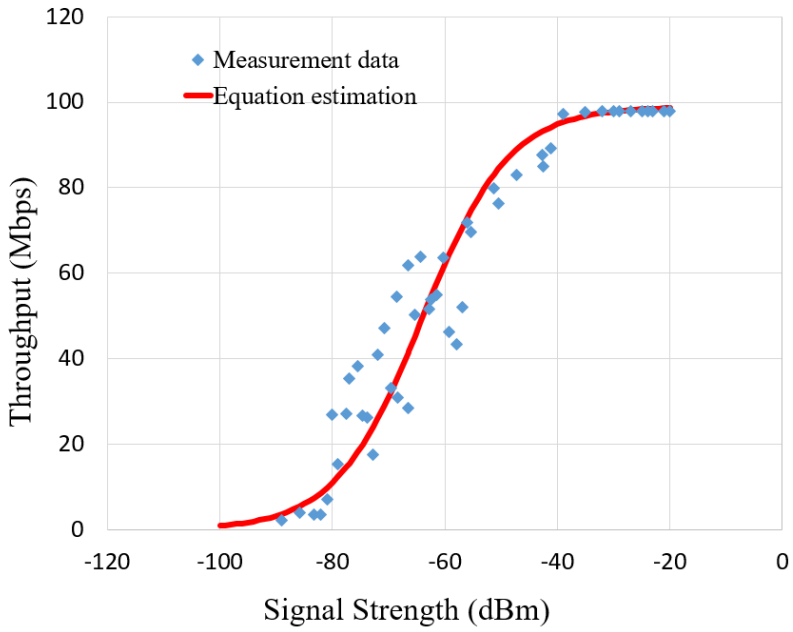

Figure 5.1: Sigmoid function for throughput estimation from signal strength.

5.5 Multipath Consideration

The RSS estimation in Section 5.3 purely considers the signal along the *line of sight (LOS)* between the AP and the host. However, due to the *multipath effect*, the signal along a different path, which is diffracted on walls, may need to be considered, particularly in an indoor environment that is a conventional target for WLAN. In this thesis, the signal along LOS is called the *direct signal* and the one along a different path is the *indirect signal* for convenience. The direct signal at the host becomes weak when several walls or obstacles exist along LOS. If the indirect signal passes only a few walls, the corresponding signal strength of the host becomes larger than the direct signal strength.

To consider the indirect signal at each host from any AP in the model, a *diffraction point* is selected for each pair of an AP and a host in the field such that it is located on a wall in the same room as the host and the RSS from the AP is largest. When no wall or obstacle exists along the

shortest path from the AP to this wall, the point that has the shortest distance from the AP is selected. However, if obstacles exist along the path, it is necessary to consider another point on a wall that has the longest distance from the AP but has a less number of obstacles, which will be investigated in future studies.

This indirect signal reaches the host in a straight line after this diffraction point, where the signal direction is changed and the signal strength is attenuated by a constant attenuation factor W_{dif}. Figure 5.2 demonstrates an example of the indirect signal through the diffraction point. It is noted that W_{dif} could be different from the direction change angle at the diffraction point, which will also be explored in future studies.

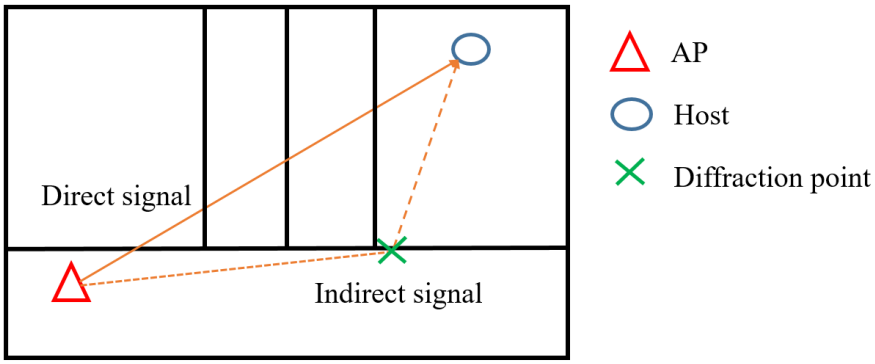

Figure 5.2: Example of indirect signal.

In our model, both the direct and indirect signal strengths are calculated for each pair of the AP and the host in the field. Then, if the indirect one is stronger than the direct one, the indirect signal strength will be used for the throughput estimation.

In a conventional model such as the *two-ray model*, it considers the phase difference of the signals, where the receiving signal strength is obtained by summing those of the direct signal and the reflected signal from the ground (indirect signal) [78].

On the other hand, our model uses either of the direct signal or the indirect signal to estimate the RSS, not the summation of them, so that it does not need to consider the phase difference of them. In other words, the accurate calculation of the phase difference is viewed as a challenging task in the indoor field that consists of multiple rooms since it requires a huge database of environmental characteristics and long simulation time. Therefore, our model adopts the simple approach of taking the stronger signal only, between the direct and indirect signals. The effectiveness of our proposal will be evaluated in Chapter 7.

5.6 Throughput Estimation Procedure

The procedure of the throughput estimation model is as follows:

(1) Calculate the Euclidean distance d (m) for each link (AP/host pair) by:

$$d = \sqrt{(AP_x - H_x)^2 + (AP_y - H_y)^2} \tag{5.3}$$

where AP_x and AP_y represent the x and y coordinates for the AP, and H_x and H_y represent the x and y coordinates for the host.

(2) Identify the walls intersecting with the link. Here, the link and the wall are regarded as line segments where their intersection is judged by considering the intersection between the two line segments.

(3) Estimate the RSS at the host using the log-distance path loss model and consider the indirect signal:

(3-a) Calculate the RSS P_{dir} at the host through the direct signal:

$$P_{dir} = P_1 - 10\alpha \log_{10} d - \sum_k n_k W_k \tag{5.4}$$

where P_{dir} represents the RSS (dBm) at the host with the distance d (m) from the AP, P_1 does the RSS (dBm) of the host with $1m$ distance from the source node, α does the distance attenuation factor that should be optimized, n_k does the number of walls with type k, and W_k does the signal attenuation factor (dB) of the type k wall.

(3-b) Calculate the RSS through the indirect signal:

1) Calculate the RSS P_{dif} (dBm) at the diffraction point for each host using (5.5).
2) Calculate the RSS P_{ind} (dBm) at the host by the indirect signal, where the RSS at 1) is used as the transmitting signal strength from the diffraction point using (5.6).

$$P_{dif} = P_1 - 10\alpha \log_{10} r - \sum_k n_k W_k \tag{5.5}$$

$$P_{ind} = P_{dif} - 10\alpha \log_{10} t - W_{dif} \tag{5.6}$$

where r (m) represents the distance between the AP and the diffraction point, t (m) does the distance between the diffraction point and the host, and W_{dif} (dB) does the attenuation factor at the diffraction point. It is observed that P_{ind} does not include the attenuation factors of the walls because the diffraction point exists in the same room as the host.

(3-c) Select the larger one between P_{dir} and P_{ind} for the RSS P_h (dBm) at the host.

(4) Calculate the estimated throughput S_h ($Mbps$) using the sigmoid function in (5.7).

$$S_h = \frac{a}{1 + \exp\left(-\frac{(120+P_h)-b}{c}\right)} \tag{5.7}$$

where a, b, and c are constant coefficients.

5.7 Host Location Selection for Measurements

The throughput estimation model has several parameters whose values must be tuned from measured throughputs: the path loss exponent factor α, the RSS at the host at the $1m$ distance from the AP P_1, and the signal attenuation factor W_k for walls with various types and the diffraction point. Thus, the following host locations must be selected for throughput measurements to tune these parameters:

(1) For each room in the field, the host location nearest from the AP should be selected to determine the path loss exponent factor, the $1m$ distance RSS, and the three sigmoid function parameters.

(2) For each wall type, the host location across the type wall from the AP should be selected to determine the attenuation factor.

(3) For each diffraction point, the host location nearest from the AP in the room should be selected to determine the attenuation factor at the diffraction point to reflect multipath effect, where the direct path from the AP passed through three or more walls.

5.8 Summary

In this chapter, we presented the throughput estimation model for the minimax AP setup optimization approach. This model consists of the receiving signal strength estimation using the log-distance path loss model and the throughput conversion using the sigmoid function, where the parameters should be tuned using measurement results. Besides, our model considers the indirect signal in addition to the direct signal for the multipath effect. Finally, the selection procedure of the host locations for throughput measurements is presented.

Chapter 6

Parameter Optimization Tool

In this chapter, we present the parameter optimization tool to optimize the parameter values for the throughput estimation model using the measurement results.

6.1 Introduction

The throughput estimation model in Chapter 5 has several parameters whose value determines the estimation accuracy. The accurate model is important for designing high-performance WLAN [79, 80, 81].

In this thesis, the parameter values of the model are optimized by use of the *parameter optimization tool*. It is implemented using the algorithm in [21, 22]. This tool has been implemented in the general form so that it can be used for a variety of algorithms/logics that have parameters to be optimized.

Normally, the program for the parameter optimization tool has been independently implemented from the program for the throughput estimation model. It runs the model program as its child process. The optimality of the current parameter values in the model program is evaluated by the throughput estimation error that is given in the output file.

6.2 Required Files for Tool

A user of the parameter optimization tool is required to prepare the following five files.

6.2.1 Parameter Specification File

The *parameter specification file* describes the condition how to change the value of each parameter during the search process. "parameter.csv" must be used as the file name. Each line in this file reflects the specification for one parameter, and must describe in the order of "parameter name", "initial value", "lower limit", "upper limit", and "change step".

The following example shows the specifications for three parameters, x, y, and z.

Example of parameter.csv.

01: $x, 50, 0, 100, 5$
02: $y, -20, -50, 0, 2$
03: $z, 0.5, 0.0, 1.0, 0.1$

6.2.2 Model Program File

The *model program file* is a binary code file to run the throughput estimation model, which could be executed through the command line. Any name is possible for this file. In addition, this file must satisfy the following two conditions:

(1) When the program is executed, it receives the path for the parameter file in the argument and applies the parameter values in the file to the model.

(2) When the program is completed, it outputs the score as the evaluation value in the text file "result.txt".

With (1), the model program can read the parameter values that are generated by the tool. With (2), the tool program can read the score that is calculated in the model program. For example, the parameter file for the previous example with three parameters is explored when their initial ones are used.

6.2.3 Sample Input Data File

The *sample input data file* contains the input data set to the model program such that the result of the program is evaluated and used to optimize the parameter values by the tool. To upgrade the accuracy of the obtained parameter values, multimodal sample input data sets should be collected and adopted in the tool.

6.2.4 Score Output File

The *score output file* involves the score from the model program to evaluate the current parameter values. The score is given by the difference between measured and estimated throughputs in the throughput estimation model.

6.2.5 Script File for Execution

The *script file* describes the sequence of the commands to execute the model program. The file name must be "run.sh". This file also describes the paths to the input files to the model program. By modifying this script file, the user is able to change the name and the arguments for the model program, and may run multiple programs sequentially to obtain one score. In the following example, line 10 executes the model program, which is coded in Java, with three paths to the input files. When the model program is executed with multiple sample input data files continuously, the array to describe these files should be prepared and the loop procedure should be adopted.

Example of "run.sh".

```
01: #!/bin/bash
02: DIR=$(cd $(dirname $0); pwd)
03: PARAMETER_FILE=$1
04: cd "$DIR"
05: #folder for sample input data files
06: INPUT_DIR="./file/3f_ap1/"
07: #measurement data file
08: MEASUREMENT_FILE="./file/evaluate/indoor_3f_ap1.csv"
09: #execute the model program
10: java -jar ThroughputEstimation.jar
${INPUT_DIR} ${MEASUREMENT_FILE}
$PARAMETER_FILE
11: #move \enquote{result.txt} to the folder containing the parameter file
12: mv result.txt ‘dirname $PARAMETER_FILE‘
```

6.3 Processing Flow of Tool

The processing flow of the tool is described as follows:

(1) The parameter optimization tool (T) generates the initial parameter file by copying the initial values in the parameter specification file.

(2) T executes the script file using the current parameter file.

(2-a) The model program (M) reads one sample input data file.

(2-b) M computes the algorithm/logic.

(2-c) M writes the score in the score output file.

(3) T reads the score from the score output file.

(4) When the termination condition is satisfied, T goes to (5). Otherwise, T goes to (6).

(5) T changes the parameter file based on the algorithm in the next section, and goes to (2).

(6) T selects the parameter values with the best score and outputs it.

6.3.1 Symbols in Algorithm

The following symbols are used in the parameter optimization algorithm in the tool:

- P: the set of the n parameters for the algorithm/logic in the model program whose values should be optimized.
- p_i: the ith parameter in P ($1 \leq i \leq n$).
- Δp_i: the change step for p_i.
- t_i: the tabu period for p_i in the tabu table.

- $S(P)$: the score of the algorithm/logic using P.
- P_{best}: the best set of the parameters.
- $S(P_{best})$: the score of the algorithm/logic where P_{best} is used.
- L: the log or cache of generated parameter values and their scores.

6.4 Parameter Optimization Algorithm

In this section, we describe the parameter optimization algorithm adopted in the *parameter optimization tool*.

6.4.1 Algorithm Procedure

The algorithm procedure that minimizes the score is described as follows:

(1) Clear the generated parameter log L.

(2) Set the initial value in the parameter file for any p_i in P, and set 0 for any tabu period t_i, and set a large value for $S(P_{best})$.

(3) Generate the neighborhood parameter value sets for P by:

(3-a) Randomly select one parameter p_i for $t_i = 0$.

(3-b) Calculate parameter values of ${p_i}^-$ and ${p_i}^+$ by:

$$
\begin{aligned}
{p_i}^- &= p_i - \Delta p_i, \text{if } p_i > \text{lower limit}, \\
{p_i}^+ &= p_i + \Delta p_i, \text{if } p_i < \text{upper limit}.
\end{aligned}
$$

(3-c) Generate the neighborhood parameter value sets P^- and P^+ by replacing p_i by ${p_i}^-$ or ${p_i}^+$:

$$
\begin{aligned}
P^- &= \{p_1, p_2, \ldots, {p_i}^-, \ldots, p_n\} \\
P^+ &= \{p_1, p_2, \ldots, {p_i}^+, \ldots, p_n\}
\end{aligned}
$$

(4) When P (P^-, P^+) exists in L, obtain $S(P)$ ($S(P^-)$, $S(P^+)$) from L. Otherwise, execute the model program using P (P^-, P^+) to obtain $S(P)$ ($S(P^-)$, $S(P^+)$), and write P and $S(P)$ (P^- and $S(P^-)$, P^+ and $S(P^+)$) into L.

(5) Compare $S(P)$, $S(P^-)$, and $S(P^+)$, and select the parameter value set that has the largest one among them.

(6) Update the tabu period by:

(6-a) Decrement t_i by -1 if $t_i > 0$.

(6-b) Set the given constant tabu period TB for t_i if $S(P)$ is largest at (5) and p_i is selected at (3-a).

(7) When $S(P)$ is continuously largest at (5) for the given constant times, go to (8). Otherwise, go to (3).

(8) When the hill-climbing procedure in (9) is applied to the given constant times HT, terminate the algorithm and output P_{best}. Otherwise, go to (9).

(9) Apply the hill-climbing procedure:

(9-a) If $S(P) < S(P_{best})$, update P_{best} and $S(P_{best})$ by P and $S(P)$ respectively.

(9-a) Reset P by P_{best}.

(9-c) Randomly select p_i in P, and randomly change the value of p_i within its range.

(9-d) Go to (3).

6.5 Summary

In this chapter, we presented a versatile parameter optimization tool to find optimal values of the parameters in the throughput estimation model. We first described five input files to be prepared, and explained them using examples. Then, we described the processing flow of the tool. Finally, we presented the parameter optimization algorithm adopted in the tool. In the next chapter, we will evaluate the effectiveness of the parameter optimization and the throughput estimation model.

Chapter 7

Evaluations for Throughput Estimation Model with Parameter Optimization Tool

In this chapter, we evaluate the throughput estimation model with the parameter optimization tool in three network fields.

7.1 Network Fields and Devices for Evaluations

The three network fields, namely field#1, field#2 and field#3 in Figure 7.1, are considered in this evaluation. The triangle in each field represents the AP and the circle does the host location. The *diffraction point* for each AP and host is manually selected. The measurement setup in Section 3.1 is adopted for the throughput measurements.

For the AP, NEC WG2600HP [53] with four internal antennas is used. For the host, a laptop PC with Windows OS is used, where Qualcomm Atheros AR9285 IEEE802.11b/g/n wireless adapter is used for SISO, Dual Band Wireless-AC 8260 wireless adapter is for 2×2 MIMO, and the 40 MHz bonded channel at 2.4 GHz is used for any link.

This AP can support the maximum transmission rate of 600 Mbps (standard value) using four streams and the 40 MHz bonded channel at 2.4 GHz for IEEE 802.11n, whereas the client PCs support the maximum transmission rate of 150 Mbps (standard value) with the bonded channel for one stream and 300 Mbps for two streams. Consequently, the maximum transmission rate for the SISO link and MIMO link between the AP and the client PC in our measurements are 150 Mbps and 300 Mbps respectively.

iperf is used as the software for throughput measurements that generates TCP traffics for 50 sec with 477 Kbytes window size and 8 Kbyte buffer size. During measurements, *iperf* is run for only one link between the server and each client host, in order to consider the single link communication for the throughput estimation model. It is noted that all the experiments were conducted on weekends to reduce the interferences from other wireless devices and human movements.

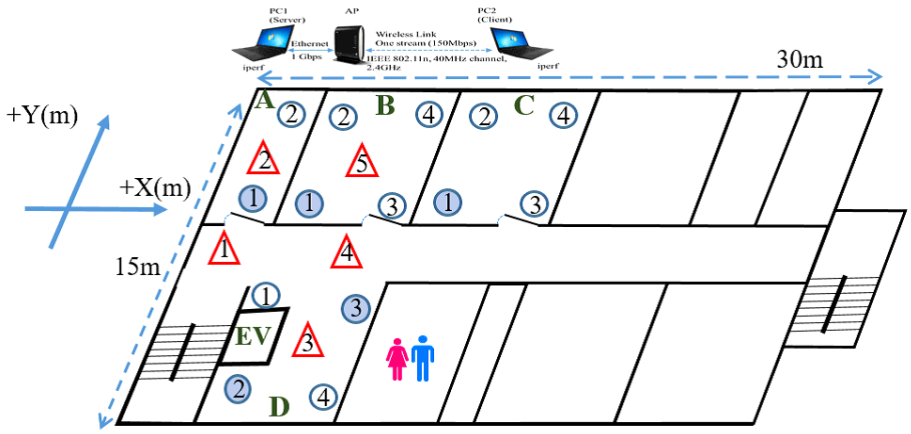

3rd Floor, Engineering Building No.2, Okayama University.

(a) Network field#1

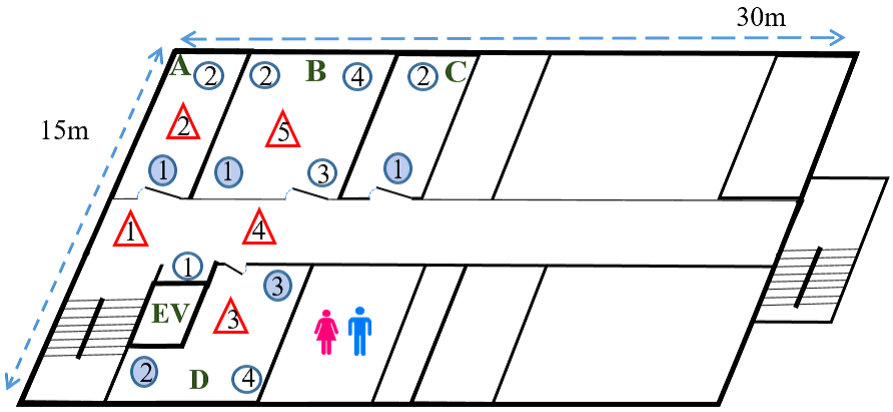

2nd Floor, Engineering Building No.2, Okayama University.

(b) Network field#2

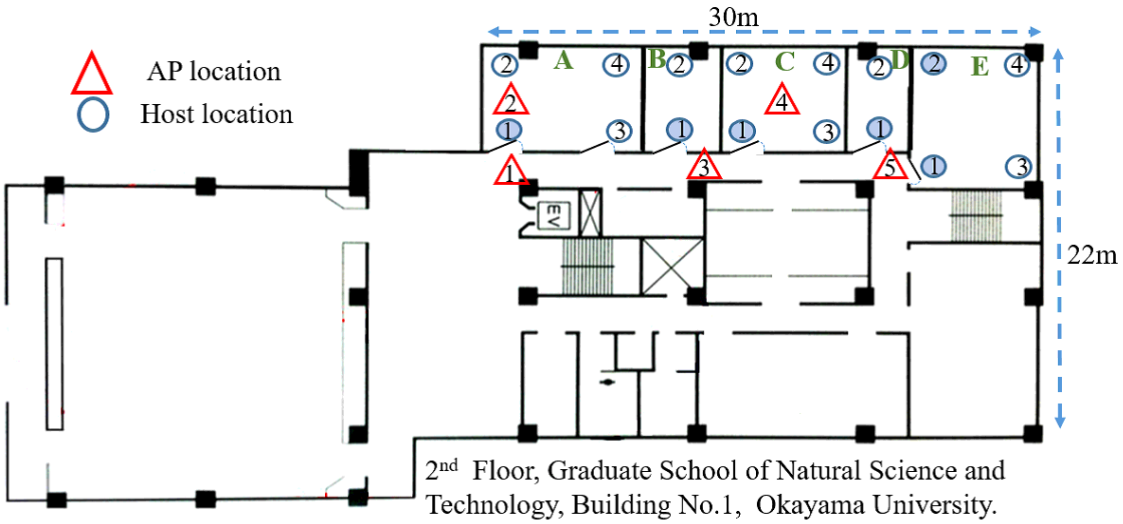

2nd Floor, Graduate School of Natural Science and Technology, Building No.1, Okayama University.

(c) Network field#3

Figure 7.1: Three network fields.

7.2 Throughput Estimation Model

In this section, the accuracy of the throughput estimation model through the application of the parameter optimization tool is evaluated. Two AP locations in the corridor are considered in each field. For throughput measurements, 14 host locations are considered in field#1, 12 locations are in field#2, and 16 locations are in field#3. Only SISO links are used for evaluations.

7.2.1 Parameter Optimization Results

First, the values of the parameters in the throughput estimation model, namely, P_1, α, W_k, and W_{dif} in (5.4), (5.6), and (5.5), and a, b, and c in (5.7) are optimized by applying the parameter optimization tool using the measured data in the three fields.

W_k is prepared for each wall type. In this evaluation, the corridor wall (W_1), the partition wall (W_2), the intervening wall (W_3), the glass wall (W_4), and the elevator wall (W_5) are examined. W_{dif} is the common attenuation factor for the diffraction points. For the parameters in the parameter optimization algorithm, $TB = 16$ and $HT = 10$ are adopted. Because field#1 and field#2 are located in the same building on different floors, all the sample input data sets measured with the four APs and 26 hosts in these two fields are used to select the optimal values of the parameters.

Table 7.1 compares the parameter values selected by manual with the direct signal only, by the tool with the direct signal only, and by the tool with the direct and indirect signals considered. The results reveal that the value of the distance attenuation factor α by the tool becomes much smaller than that by manual. For manual, the measured data sets in the open space were used, whereas for the tool, the data sets in the indoor spaces were used, which indicates that α is small in indoor environments. The wall attenuation factor W_k is larger for the stronger wall.

Table 7.1: Parameter optimization results.

para-meter	field#1,2			field#3		
	manual direct	tool direct	tool indirect	manual direct	tool direct	tool indirect
P_1	-20.0	-35.0	-35.0	-20.0	-37.0	-35.1
α	3.20	2.76	2.60	3.20	2.10	2.00
W_1	15.0	12.9	12.5	8.0	14.3	16.4
W_2	6.0	3.0	3.0	3.0	2.0	3.6
W_3	12.0	7.0	6.5	-	-	-
W_4	3.0	4.0	4.0	-	-	-
W_5	6.0	3.9	4.0	-	-	-
W_{dif}	-	-	2.9	-	-	2.0
a	80.0	74.8	73.8	98.0	105.0	103.0
b	50.0	45.4	47.0	50.0	40.5	40.1
c	4.00	6.05	5.48	4.00	7.28	6.75

7.2.2 Throughput Estimation Results

Subsequently, the whole throughput estimation model is applied using the parameter values in Table 7.1. Table 7.2 summarizes the average, maximum, minimum, and standard deviation (SD) of the scores or throughput estimation errors (Mbps) on the links between the hosts and each AP in the three fields. For reference, Figure 7.2 displays the measured and estimated throughputs for the hosts in field#1, field#2 and field#3 respectively.

In Figure 7.2, the throughput measurement results are compared with three estimation results, namely *manual*, *tool (old model)*, and *tool (new model)*. In *manual*, the old model, which indicates no use of the indirect signal, is adopted, and the parameter values are tuned manually. In *tool (old model)*, the old model is adopted, and the parameter values are tuned by the tool. In *tool (new model)*, the new model, which indicates the use of the indirect signal, is adopted, and the parameter values are tuned by the tool. The *old model* uses simply the direct signal for any link between an AP and a host to estimate the throughput. The *new model* selects the indirect signal if the receiving signal strength becomes stronger than that of the direct signal, to consider the *multipath effect*.

In Figure 7.2, no difference exist between *tool (old model)* and *tool (new model)* in terms of the throughput of bottleneck hosts in field#1 and field#2, because the direct signal is dominant in the link for any host including the bottleneck host. This reason could originate from the fact that the number of passing walls is at most three for any link. For these fields, the parameter optimization tool generally improves the throughput estimation accuracy, which confirms the effectiveness of the tool.

In field#3, the direct signal from AP1 needs to pass through five walls to reach hosts E-2 and E-4 in room E. Then, the estimated throughputs for these hosts using the direct paths become much lower than the measurement results. Consequently, E-2 is selected as the bottleneck host in *manual* and *tool (old model)*, although D-2 has been shown as a bottleneck host from the measurement results.

In the new model, the indirect signal is used to estimate the throughput for hosts E-2 and E-4, where this signal passing through only one wall is diffracted at a diffraction point on the wall in room E, and the receiving signal strength is larger than that of the direct signal passing through five walls. This consideration of the indirect signal improves the throughput estimation accuracy for these two hosts, and correctly selects D-2 for the bottleneck host in field#3 by *tool (new model)*. It is critical to clarify the conditions that the new model has functioned well, which will be explored in future studies.

Table 7.2 indicates that the accuracy of the throughput estimations by the model is generally improved by the tool. The accuracy for the two hosts, E-2 and E-4, with AP1 in field#3, is greatly improved by considering the indirect signal. These results have verified the contributions of the parameter optimization tool and the indirect signal consideration to improve the estimation accuracy.

However, the standard deviation of the estimation errors is increased for AP1 and AP4 in field#1. Figure 7.2 shows that the errors of A-1, A-2, and D-1 for AP1 and the errors of D-1 and D-4 for AP4 are prominently increased by the model and become much larger than the errors for other hosts. From Figure 7.1, these hosts are located quite close to the corresponding AP, which means that our model for a link between an AP and its nearby host is not sufficient. The further improvements of the model, particularly for short links, will be studied in future works.

Table 7.2: Throughput estimation errors (Mbps).

field	AP	method	model	average	maximum	minimum	SD
field#1	AP1	manual	direct	9.42	18.7	0.62	6.46
		tool	direct	7.04	26.6	0.0	8.54
		tool	indirect	6.93	26.6	0.11	8.49
	AP4	manual	direct	11.4	26.0	0.58	8.42
		tool	direct	9.29	24.6	0.1	9.06
		tool	indirect	9.11	25	0.02	9.07
field#2	AP1	manual	direct	19.1	34.6	5.07	9.95
		tool	direct	11	19	3.2	5.20
		tool	indirect	11	18.9	3.4	5.04
	AP4	manual	direct	18.7	31.8	4.96	8.39
		tool	direct	8.83	15.5	1.75	4.19
		tool	indirect	8.96	15.4	2.46	4.17
field#3	AP1	manual	direct	13.2	38.2	0.83	11.16
		tool	direct	6.79	19.3	0.0	5.46
		tool	indirect	4.65	12.2	0.04	4.19
	AP5	manual	direct	16.36	38.96	4.18	9.58
		tool	direct	8.57	20.91	0.05	5.80
		tool	indirect	5.29	16.14	0.01	4.77

7.2.3 Bottleneck Host Detection Results

In any AP location, the bottleneck host providing the lowest measured throughput is coincident with the one found by the model. Specifically, in field#1, C-4 is the bottleneck host for AP1 and A-2 is for AP4. In field#2, C-2 is for AP1 and A-2 is for AP4. In field#3, D-2 is for AP1 and A-2 is for AP5. These outcomes support the use of the throughput estimation model to identify the bottleneck host that will be used in the following AP setup optimization.

It is assumed that only one AP has existed in the field until now, although it is more natural that two or more APs exist there. As a straightforward extension of our proposal to multiple APs, for each host, the throughput from each AP is estimated using the model, and the associated AP is selected by detecting the largest throughput. Then, the bottleneck host is selected for each AP in the field such that the estimated throughput is the smallest among the associated hosts.

However, this straightforward extension does not consider the load imbalance between the APs in the field. If the load imbalance occurs, the associated AP for a host could be different and the bottleneck host may be changed. The consideration of the load imbalance in detecting bottleneck hosts for multiple APs will be included in future studies.

Figure 7.3 reveals the estimated throughputs by *tool (new model)* for each host from AP1 and AP4 in field#1. AP1 is selected for the associations of the four hosts A-1, A-2, B-1, and D-1, whereas AP4 is selected for the other 10 hosts. That is, if the straightforward extension will be applied to this field, A-2 is the bottleneck for AP1 and C-4 is for AP4. The throughput of this bottleneck host for AP1 is much larger than that for AP4. Therefore, it is noticed that the consideration of the load imbalance among the two APs is critical in this field.

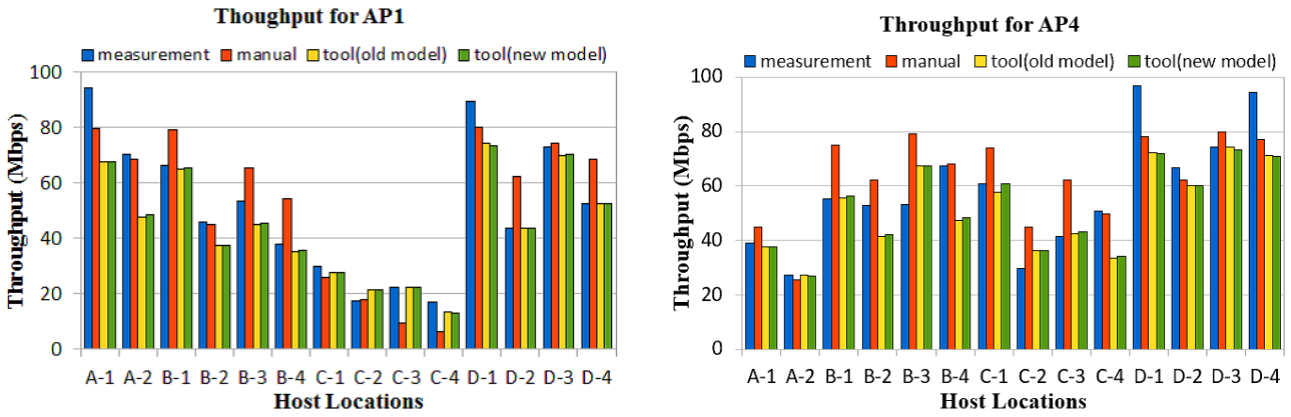

(a) Throughput results in field#1

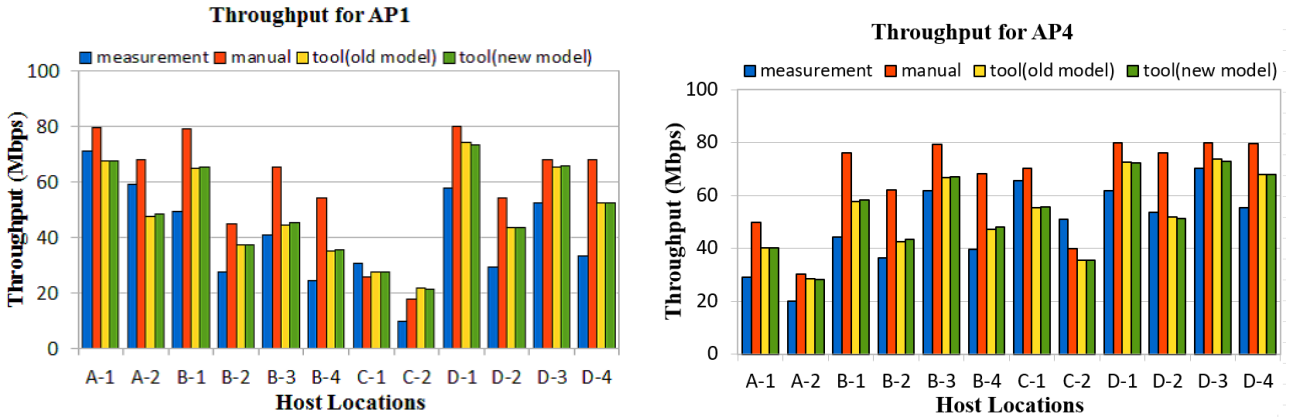

(b) Throughput results in field#2

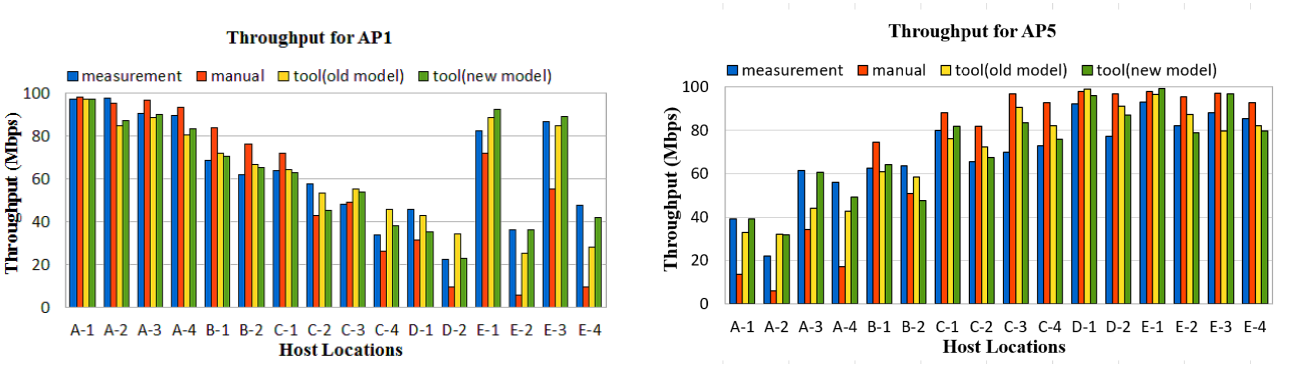

(c) Throughput results in field#3

Figure 7.2: Measured and estimated throughput results.

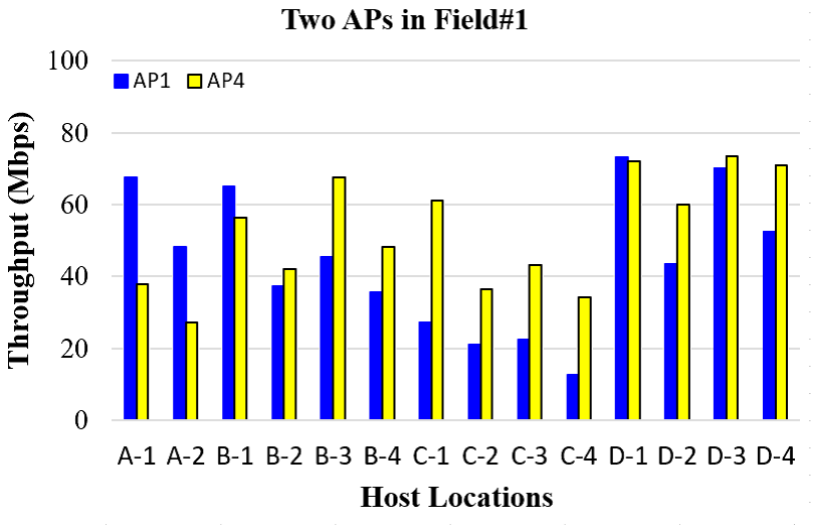

Figure 7.3: Throughputs for two APs in field#1.

7.3 Host Location Selection for Minimal Throughput Measurements

In this section, we evaluate the host location selection procedure for minimal throughput measurements in parameter optimizations.

7.3.1 Selected Host Locations for Minimal Throughput Measurements

The host locations for minimal throughput measurements in Section 5.7 are selected in the three fields. Particularly, five host locations are selected in field#1 and field#2, and six host locations are in field#3. For example, the shaded circle in Figure 7.1 indicates the selected host location for AP1 respectively.

7.3.2 Parameter Optimization Results

First, the values of the parameters in the model, P_1, α, W_k, W_{dif}, a, b, and c, are optimized by applying the parameter optimization tool using the measured data in each field. As the wall types, the corridor wall (W_1), the partition wall (W_2), the intervening wall (W_3), the glass wall (W_4), the elevator wall (W_5), and the door (W_6) are examined. W_{dif} is the common attenuation factor for the diffraction points. To improve the estimation accuracy, α_{inc} (enhanced path loss exponent factor) for $d \geq d_{thr}$ (distance threshold) is also considered.

Tables 7.3 and 7.4 compare the parameter values that were obtained by applying the parameter optimization tool to the measurement results at all the host locations (*all*) and to those at the selected locations by the proposal (*proposal*) for each AP using SISO links and MIMO links respectively. They reveal that the values of the path loss exponent and the attenuation factors are similar between *all* and *proposal*. The validity of the host locations for throughput measurements in Section 5.7 is confirmed.

7.3.3 Throughput Estimation Results

Then, the throughput is estimated by using the throughput estimation model with the parameter values in Table 7.3 for SISO links and Table 7.4 for MIMO links. To verify the accuracy of the model, the throughput estimation errors (Mbps) that are given by the difference between the measured ones and the estimated ones are calculated.

Tables 7.5 and 7.6 summarize the average, maximum, minimum, and standard deviation (SD) of them for all the links between the host locations and each AP. In any field, the estimation accuracy of the model is kept similar by *all* and *proposal* with both SISO and MIMO links, which indicates that the accuracy of the model is not lowered with fewer measurements by the proposal. Thus, the effectiveness of our proposal in reducing labor costs is confirmed.

In field#3, the estimation accuracy is better than other two fields, because a fewer obstacles such as tables, bookshelves, and equipment exist there. The estimation accuracy of SISO links is higher than that of MIMO links, because of the use of the *sigmoid function* in the throughput estimation model. The throughput of the 2×2 MIMO link becomes the double of that of the SISO link, whereas the RSS range is the same [82]. As a result, the estimated throughput can be widely changed even if the RSS is slightly changed. Thus, even a small error of RSS can magnify the error of the estimated throughput.

Table 7.3: Parameter optimization results for SISO.

parameter	field#1		field#2		field#3	
	# measured hosts		# measured hosts		# measured hosts	
	all	proposal	all	proposal	all	proposal
P_1	-35.9	-35.8	-37.6	-37.7	-34	-35.1
α	2.00	2.00	2.00	2.00	2.00	2.00
α_{inc}	2.10	2.10	2.10	2.10	2.04	2.01
d_{thr}	5	5.2	6.5	5.2	5	5
W_1	7	7	7	7	8	6
W_2	7	8	7	7	5	4
W_3	8	8	10	9	-	-
W_4	-	-	2	2	-	-
W_5	2.9	2	2.8	2.0	-	-
W_6	2	3	5.0	3.7	2	2.8
W_{dif}	2	2	2	2	3.1	2
a	90	90	85	85	98	94
b	55	53.5	50	52	40	44.5
c	8	8	8	8	7.5	8

Table 7.4: Parameter optimization results for MIMO.

parameter	field#1		field#2		field#3	
	# measured hosts		# measured hosts		# measured hosts	
	all	proposal	all	proposal	all	proposal
P_1	-34.0	-35.6	-36.2	-35.2	-35.2	-34
α	2.39	2.09	2.31	2.20	2.00	2.10
α_{inc}	2.49	2.19	2.41	2.40	2.10	2.20
d_{thr}	5	5	7	5.2	6.3	5
W_1	7	7	7	7	7	7
W_2	8	8	8	8	5	5
W_3	7	7	7	7	-	-
W_4	-	-	3.0	2	-	-
W_5	2	2	3.2	2.8	-	-
W_6	4.7	3	3.7	3	2	2
W_{dif}	1.9	2	1.5	2	2	1.9
a	190	190	190	190	195	194
b	47	46.5	47.5	50	40	40
c	6.5	7	6	8	6.5	6.5

Figure 7.4 shows the measured throughput, the estimated one using all the host locations, and the estimated one using the selected host locations at every host location for AP1 in field#1. It shows the similarity between them.

Table 7.5: Throughput estimation errors (Mbps) for SISO.

field	AP	para. set	average	max	min	SD
field#1	AP1	all	5.72	14.11	0.01	4.44
		proposal	7.04	15.80	1.21	4.28
	AP4	all	9.55	24.86	0.53	7.73
		proposal	8.83	26.76	0.46	8.12
field#2	AP1	all	12.19	22.92	1.05	7.89
		proposal	11.52	20.85	0.21	6.35
	AP4	all	9.53	18.38	3.49	5.79
		proposal	8.66	25.37	0.31	8.36
field#3	AP1	all	7.29	12.91	1.88	3.36
		proposal	7.32	13.08	0.09	3.50
	AP5	all	7.45	19.84	0.24	6.79
		proposal	7.59	19.09	1.38	6.54

Table 7.6: Throughput estimation errors (Mbps) for MIMO.

field	AP	para. set	average	max	min	SD
field#1	AP1	all	12.48	25.66	0.24	7.83
		proposal	11.83	36.58	2.11	8.65
	AP4	all	9.09	18.18	0.30	5.67
		proposal	8.61	24.82	0.39	6.94
field#2	AP1	all	12.01	20.82	3.26	6.46
		proposal	15.78	24.64	3.92	6.34
	AP4	all	10.27	19.96	1.85	6.59
		proposal	12.29	20.46	2.58	6.65
field#3	AP1	all	10.16	16.12	0.42	4.40
		proposal	12.18	20.32	0.01	5.59
	AP5	all	9.74	21.55	0.53	6.94
		proposal	9.69	24.80	0.24	7.54

7.3.4 Bottleneck Host Results

Finally, the bottleneck host detection for each AP is verified from Figures 7.5 and 7.6. In any AP location, the bottleneck host providing the lowest estimated throughput by the proposal is coincident with the one found by the measurements and by the model using all the host locations. Specifically, in field#1, C4 is the bottleneck host for AP1 and A2 is for AP4. In field#2, C2 is for AP1 and A2 is for AP4. In field#3, D2 is for AP1 and A2 is for AP5.

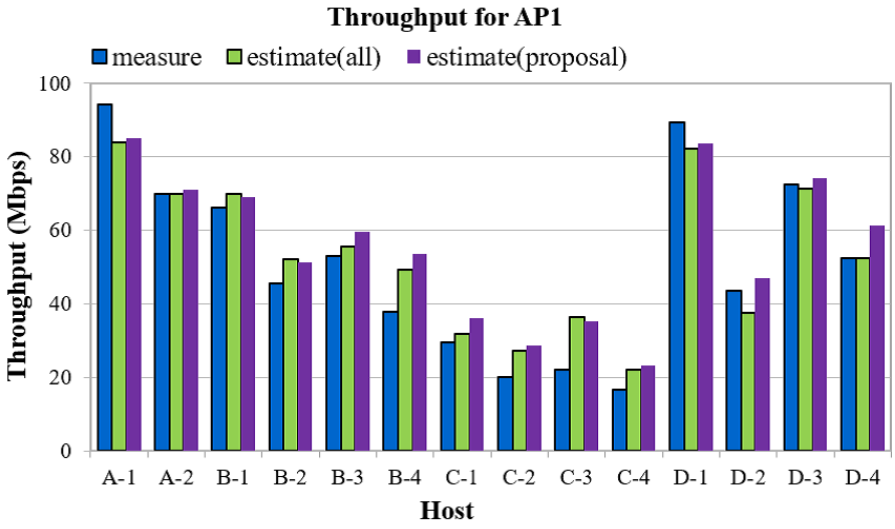

(a) SISO.

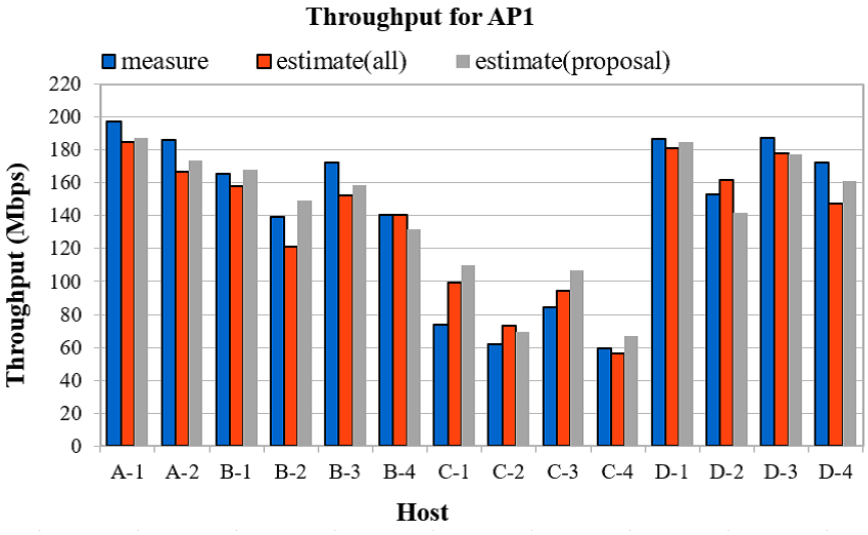

(b) MIMO.

Figure 7.4: Measured and estimated throughputs for AP1 in field#1.

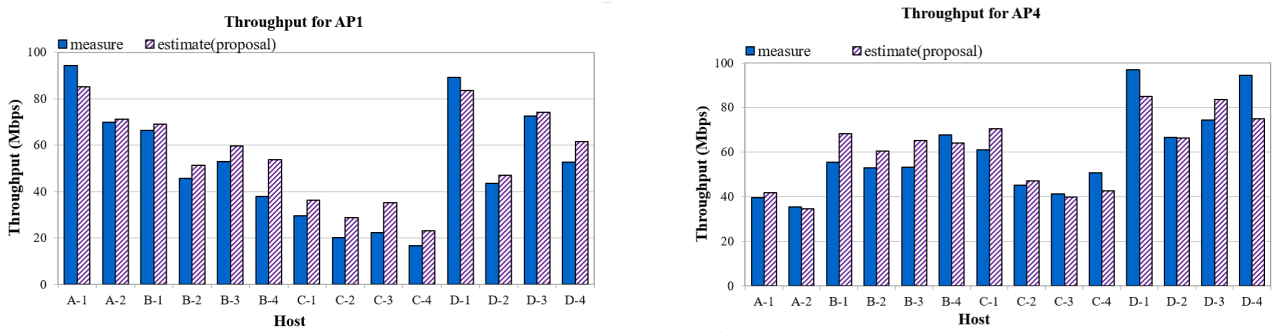

(a) Throughput results in field#1

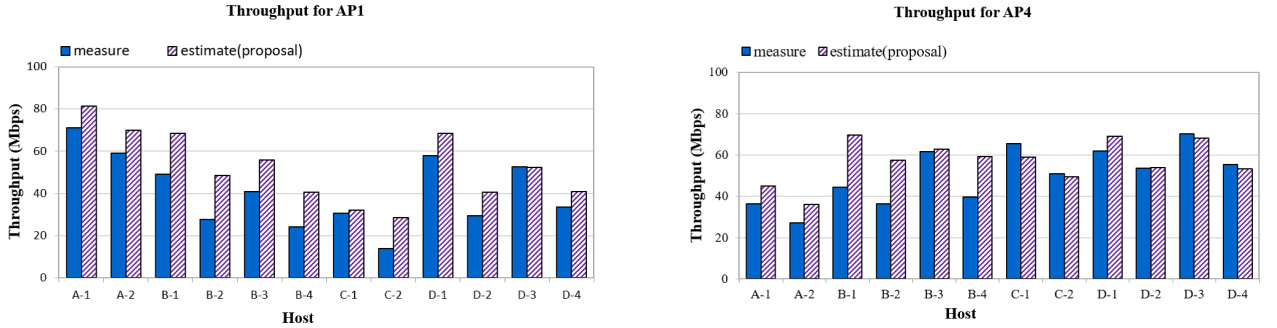

(b) Throughput results in field#2

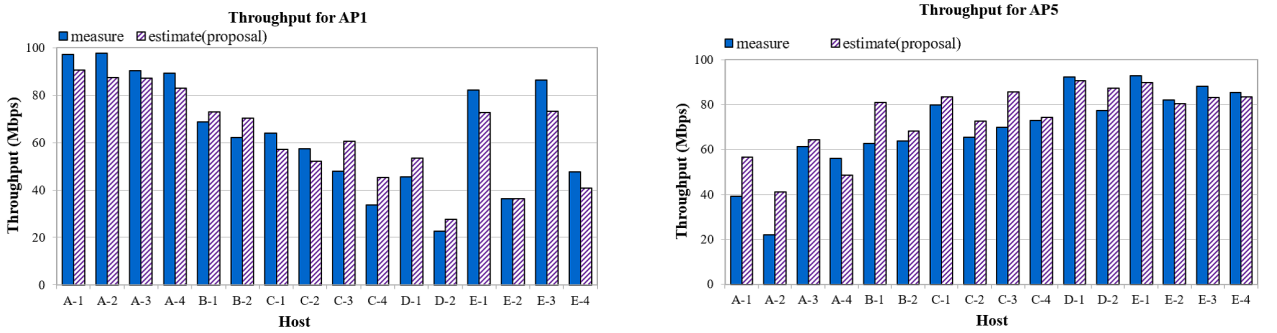

(c) Throughput results in field#3

Figure 7.5: Measured and estimated throughput results for SISO links.

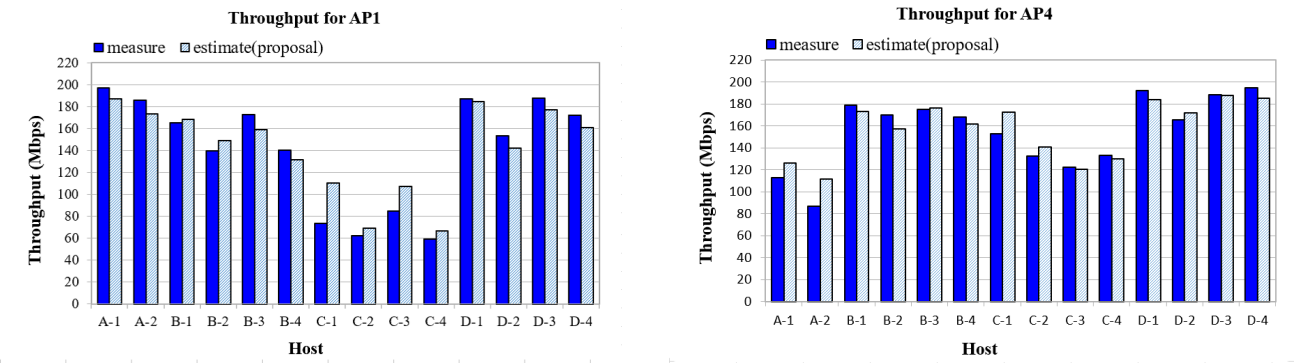

(a) Throughput results in field#1

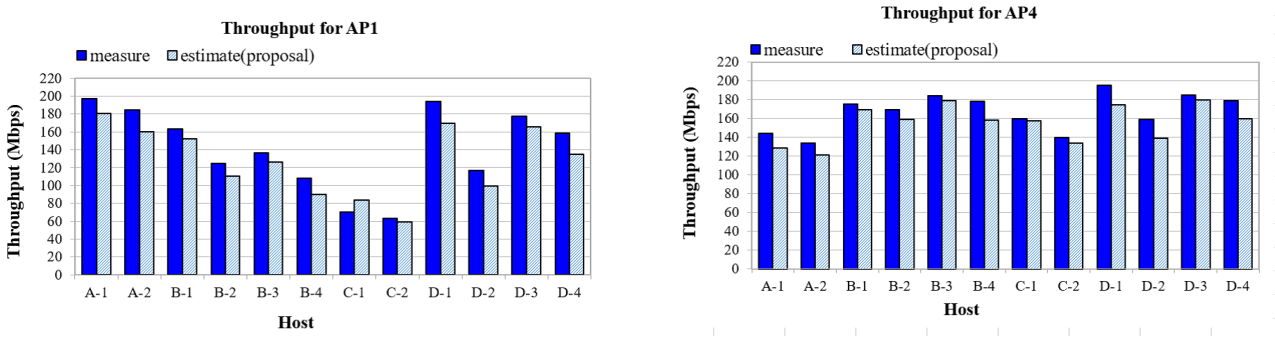

(b) Throughput results in field#2

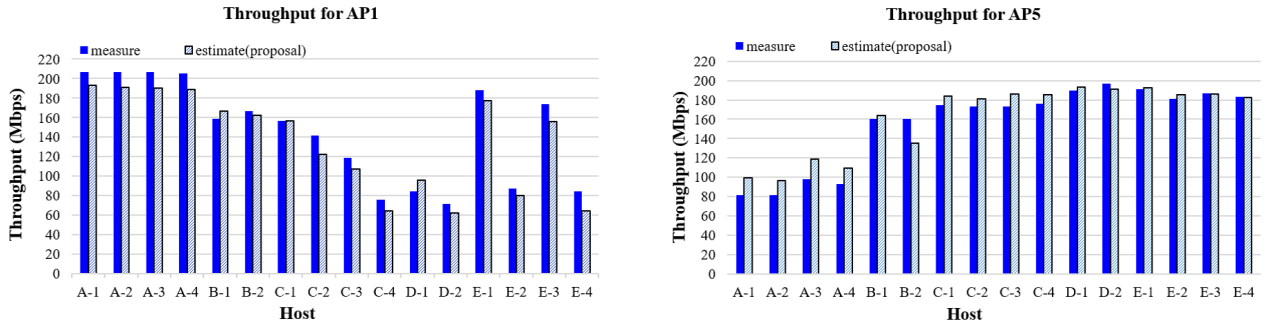

(c) Throughput results in field#3

Figure 7.6: Measured and estimated throughput results for MIMO links.

7.4 Summary

In this chapter, first, we verified the effectiveness of the proposed throughput estimation model with the use of the parameter optimization tool. We examined the accuracy of the throughput estimation model by comparing the estimated throughputs with the measurement results. Then, we evaluated the host location selection procedure for the throughput measurements. The results show that the same bottleneck host is found by the model and the measurements for any AP in the three fields. Thus, the effectiveness of our proposals is confirmed.

Chapter 8

Evaluations for Access-Point Setup Optimization

In this chapter, we evaluate the access-point setup optimization approach in three network fields.

8.1 Orientation and Height Optimization for AP Setup

The AP setup is optimized by manually changing the orientation and height of the AP to increase the measured throughput between the AP and the corresponding bottleneck host found in Chapter 7. To evaluate of the proposed AP setup optimization approach, AP1 in field#1, AP4 in field#2, and AP1 in field#3 in Figure 8.1 are considered with SISO links. First, the orientation of each AP is optimized with respect to the roll angle and the yaw angle. Then, the height of the AP is optimized by changing the number of shelves to put the AP. After that, the overall throughput improvement is evaluated for all the hosts in each network field by the AP setup optimization.

8.1.1 Orientation Optimization

First, the orientation of the AP is optimized by rotating the AP from $-90°$ to $+90°$ with the $30°$ interval along the roll and yaw axes. The pitch angle optimization was not considered, because no improvement has been observed in preliminary experiments. From the internal antenna layout of this AP in Figure 2.11, the change of the pitch angle is equivalent to the change of the height. During the following roll angle and yaw angle optimizations, the height of the AP was fixed at $1.35m$ in the field#1 and field#3, and at $0.9m$ in the field#2, as the best heights found in Section 8.1.2.

8.1.1.1 Roll Angle Optimization

Figure 8.2 shows the throughput measurement results for different roll angles in the three fields. It indicates that $90°$ roll angle provides the highest throughput of the bottleneck host in the three fields. To elaborate, the throughput increases to 38 Mbps in field#1, 37 Mbps in field#2, and 43 Mbps in field#3. On the other hand, $0°$ provides the lowest throughput of 17 Mbps in field#1, $-60°$ does the lowest one of 18 Mbps in field#2, and $-30°$ does the lower one of 19 Mbps in field#3. The highest throughput becomes more than twice of the lowest one. Thus, the optimization of the setup roll angle of the AP is critical for the throughput performance.

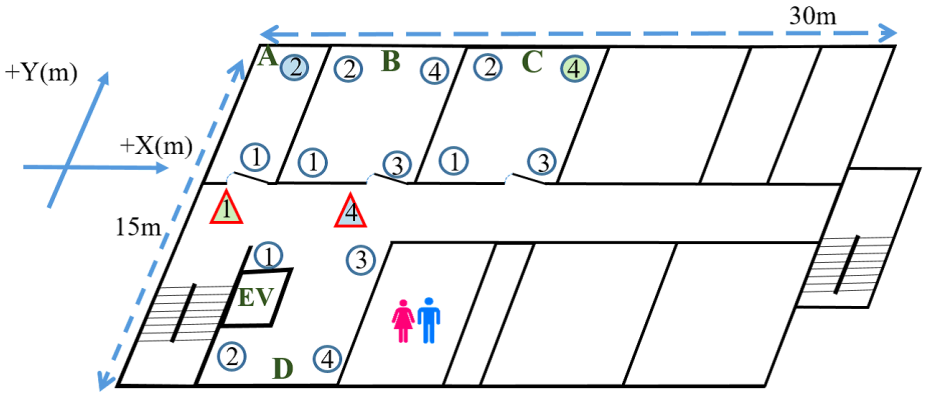

3rd Floor, Engineering Building No.2, Okayama University.

(a) Network field#1

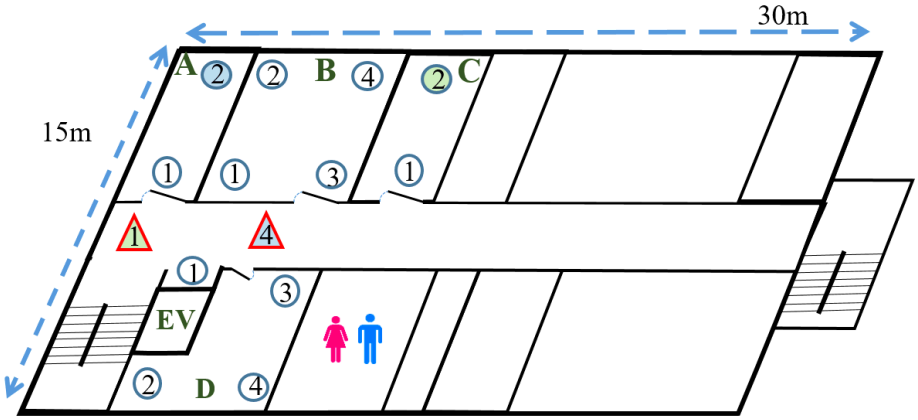

2nd Floor, Engineering Building No.2, Okayama University.

(b) Network field#2

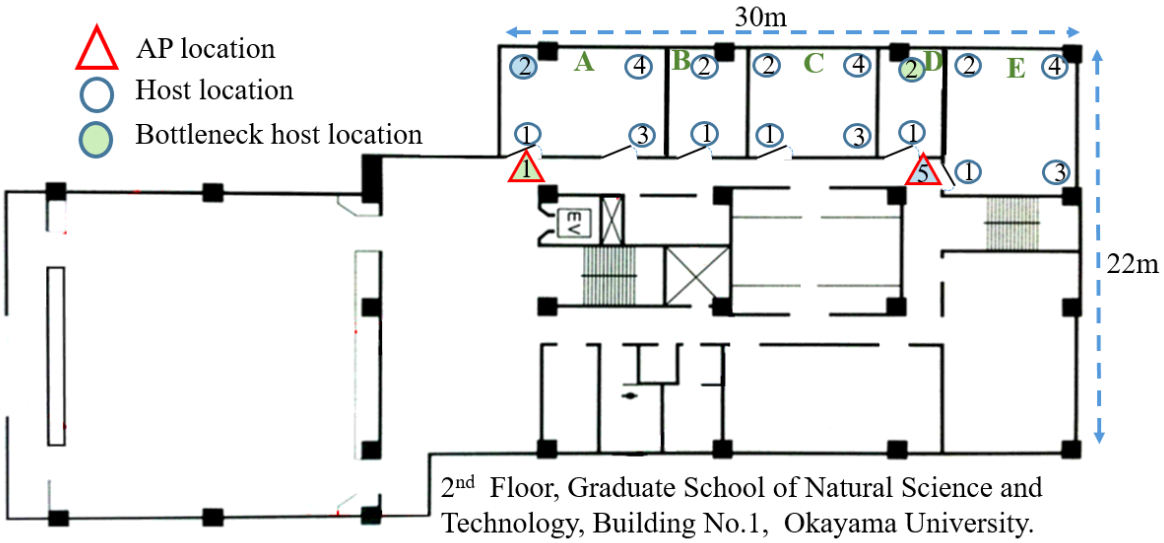

2nd Floor, Graduate School of Natural Science and Technology, Building No.1, Okayama University.

(c) Network field#3

Figure 8.1: Three network fields for AP setup optimization.

8.1.1.2 Yaw Angle Optimization

Figure 8.3 demonstrates the throughput measurement results for different yaw angles in the three fields. It indicates that the 0° yaw angle provides the highest throughput of the bottleneck host in the three fields. In details, the throughput increases to 38 Mbps in field#1, 37 Mbps in field#2, and 43 Mbps in field#3. On the other hand, 90° provides the lowest throughput of 28 Mbps in field#1, −30° does the lowest one of 20 Mbps in field#2, and 30° provides the lowest one of 28 Mbps in field#3. It means the highest throughput is more than 30% higher than the lowest one. Thus, the optimization of the setup yaw angle of the AP is extremely important as well.

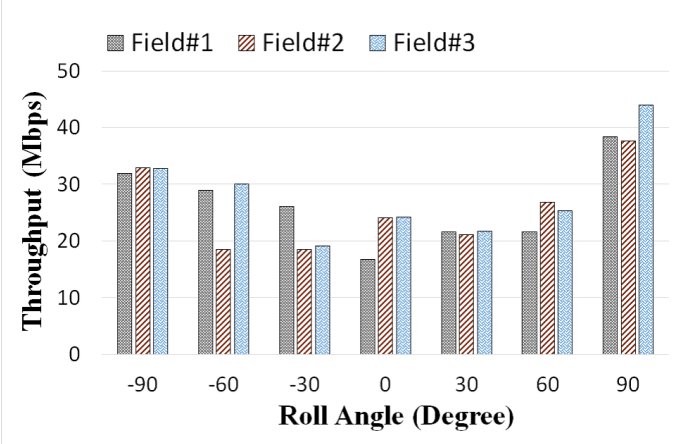

Figure 8.2: Bottleneck host throughputs for different roll angles.

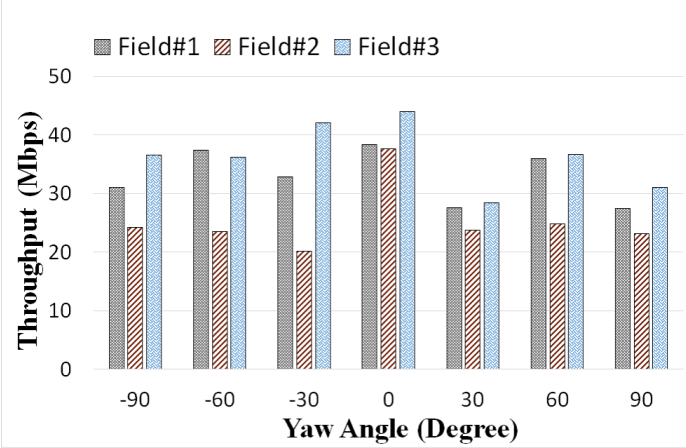

Figure 8.3: Bottleneck host throughputs for different yaw angles.

8.1.2 Height Optimization

Then, the height of the AP is optimized by changing it from $0m$ up to $1.80m$ with the $0.45m$ interval. To change the height, plastic shelves were used. It is noted that the ceiling height of each field is $2.4m$. During the height optimization, the roll/yaw angles of the AP were fixed at the best ones found in Sections 8.1.1.1 and 8.1.1.2.

Figure 8.4 unveils the throughput measurement results for different AP heights in the three fields. It conveys that 1.35m provides the highest throughput of the bottleneck host in the field#1 and field#3, and 0.9m does in field#2. Specifically, the throughput increases to 38 Mbps in field#1, 37 Mbps in field#2, and 43 Mbps in field#3. On the other hand, 0m provides the lowest throughput of 13 Mbps in field#1 and of 29 Mbps in field#3, and 1.8m does the lowest one of 24 Mbps in field#2. It implies the highest throughput is more than 30% higher than the lowest one. Likewise, the optimization of the setup height of the AP plays a principal role in the experiment.

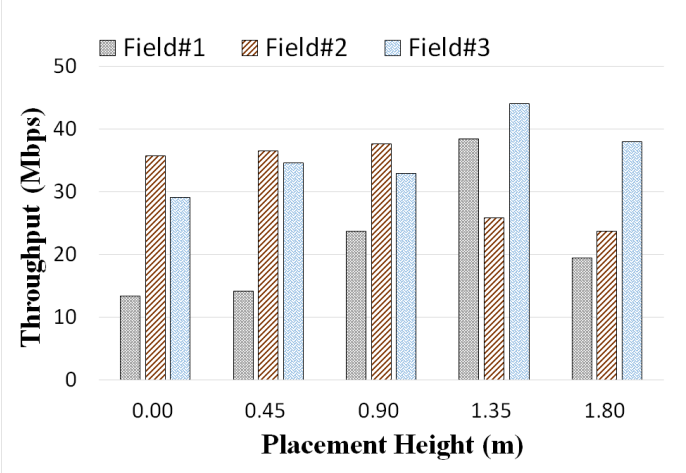

Figure 8.4: Bottleneck host throughputs for different heights.

8.2 Overall Host Throughput Improvements

Finally, the overall throughput improvement among the hosts in each network field by the AP setup optimization is evaluated. Figure 8.5 shows the throughput of each host in the three fields before and after the setup optimization. Table 8.1 summarizes the average throughput improvements by the proposed AP setup optimization for the six AP locations in the three network fields. These results reflect the fact that the proposal is qualified to improve the average throughput in any field and the individual throughput for most of the hosts. Specifically, for AP1 in field#2, the average throughput is improved from 40.48 Mbps to 52.88 Mbps, which means 30.66% improvement.

Table 8.1: Average throughput improvements.

field	AP	before Opt. (Mbps)	after Opt. (Mbps)	improvement (%)
field#1	AP1	51.06	65.23	27.77
	AP4	57.90	67.29	16.22
field#2	AP1	40.48	52.88	30.66
	AP4	49.09	52.13	6.28
field#3	AP1	64.26	70.42	9.59
	AP5	69.55	78.63	13.05

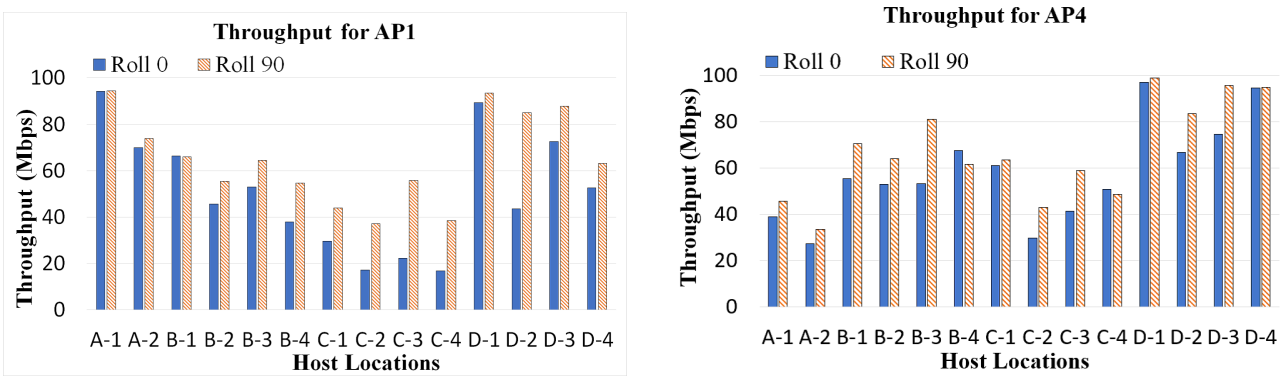

(a) Network field#1

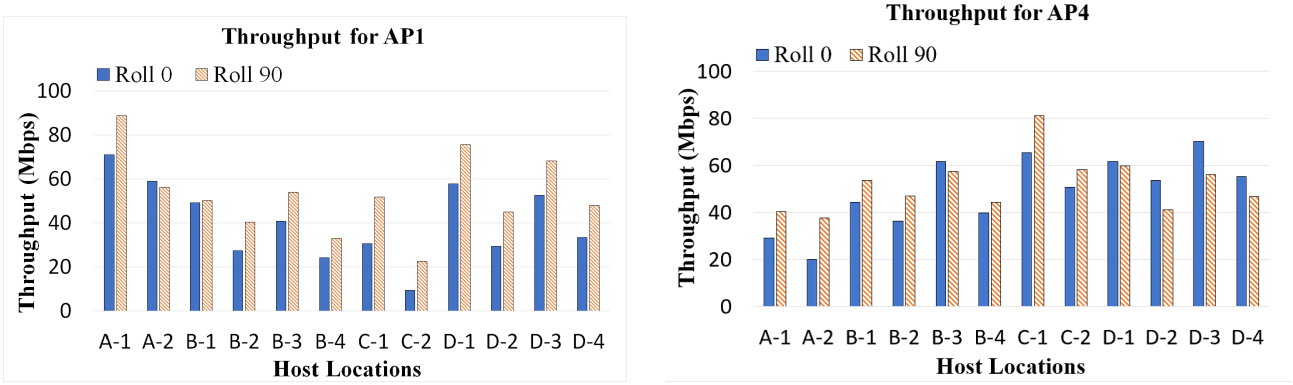

(b) Network field#2

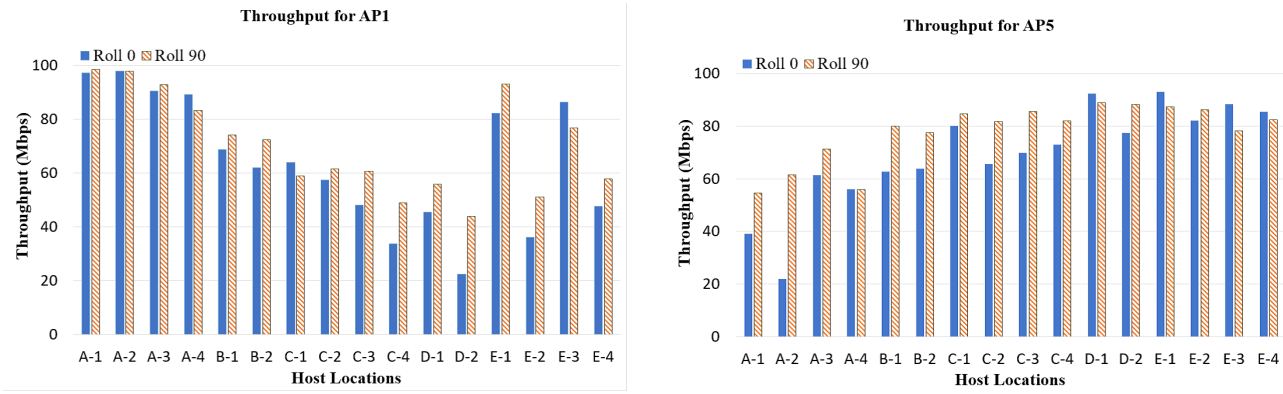

(c) Network field#3

Figure 8.5: Throughput improvements by setup optimizations.

8.3 Coordinate Shift Optimization for AP Setup

In this section, we present the *coordinate shift* as another optimization parameter in the AP setup optimization.

8.3.1 Effect of Coordinate Shift

The improvement of the *multipath effect* is important to improve the performance of a wireless communication link. It can be changed by the surrounding environment of the AP in the field. Even if the AP is shifted slightly, it may drastically change the multipath effect and affect the performance. To consider the limitation of the possible AP location due to the power supply or the available space, it is assumed that any AP can be sifted by $\pm 0.3m$ or $\pm 0.5m$ along the x or y axis from the original coordinate as shown in Figure 8.6 (b).

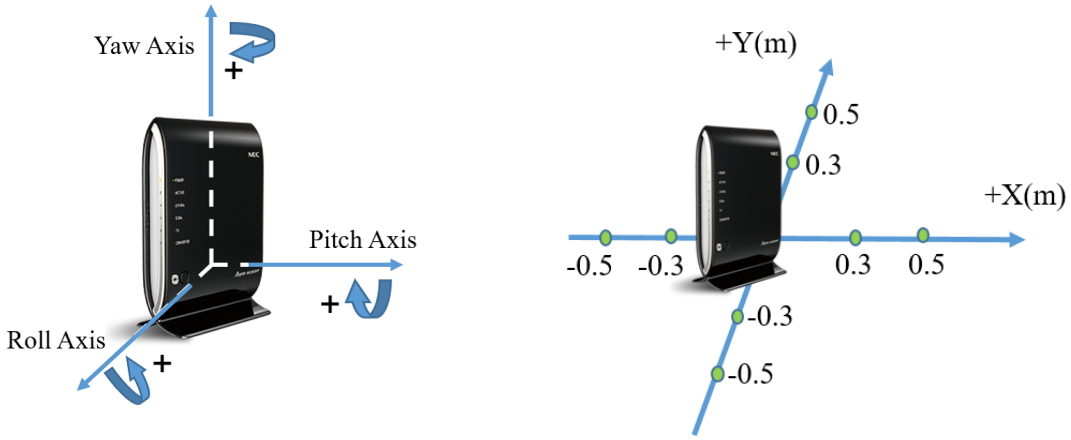

(a) Orientation axes.

(b) Coordinate shift axes.

Figure 8.6: Setup optimization parameters.

8.3.2 Coordinate Shift Results for Bottleneck Hosts

The coordinate of the AP is manually shifted by $\pm 0.3m$ or $\pm 0.5m$ along the x or y axis from the original coordinate, where the throughput of the link between the bottleneck host and the AP at each location is measured. Tables 8.2 and 8.3 show the throughput results respectively. The results indicate that the throughput can be improved by shifting the coordinate up to $0.5m$ along each axis, especially in the x-axis. The reason is that these APs are located in the corridor that is like a tunnel, and the signal can strongly propagate along the corridor. Besides, the rooms exist on both side of the corridor along the x-axis. Therefore, the coordinate shifting of AP along the corridor or x-axis can improve the throughput of the bottleneck hosts. In these fields, if the AP is shifted along the y-axis, it is closer to the center of the corridor. Therefore, the optimization of the coordinate shift in the AP setup can improve the performance.

Table 8.2: Throughputs with respect to x-axis shift.

field	AP	Throughput with respect to x-axis shifting					
		X-axis(m)	-0.5	-0.3	0	0.3	0.5
field#1	AP1	TP.(Mbps)	33.50	35.30	37.08	32.40	30.90
	AP4	TP.(Mbps)	48.00	39.90	33.32	42.80	35.00
field#2	AP1	TP.(Mbps)	27.10	27.00	22.68	12.40	34.00
	AP4	TP.(Mbps)	36.60	28.40	37.66	53.50	26.50
field#3	AP1	TP.(Mbps)	44.60	45.80	43.97	37.60	49.70
	AP5	TP.(Mbps)	43.20	46.00	61.50	47.40	37.50

Table 8.3: Throughputs with respect to y-axis shift.

field	AP	Throughput with respect to y-axis shifting					
		Y-axis(m)	-0.5	-0.3	0	0.3	0.5
field#1	AP1	TP.(Mbps)	36.10	20.40	37.08	28.30	30.90
	AP4	TP.(Mbps)	42.60	30.52	33.32	36.40	32.40
field#2	AP1	TP.(Mbps)	46.70	26.00	22.68	36.90	34.20
	AP4	TP.(Mbps)	39.00	43.20	37.66	37.50	26.40
field#3	AP1	TP.(Mbps)	47.60	49.60	43.97	45.10	41.40
	AP5	TP.(Mbps)	48.10	56.20	61.50	33.50	43.70

8.3.3 Coordinate Shift Results for All Hosts

The average throughput improvement of all the hosts by the coordinate shift is evaluated for each network field. The average throughputs of the three cases, namely, 1) the original setup, 2) before and 3) after the coordinate shift optimization with the optimized orientation and height, are compared, where the improvement rates from 1) to 2), and those from 2) to 3) are calculated. Table 8.4 shows the results for SISO links and Table 8.5 shows them for MIMO links.

These tables indicate that the coordinate shift optimization can further improve the average throughput in any field. Specifically, for AP4 in field#2 for SISO links, the average throughput is improved from 52.17 Mbps to 69.60 Mbps. However, in some APs, the coordinate shift does not improve the throughput at all. In general, the coordinate shift does not much improve the throughput for MIMO links, because using the multiple antennas, the multipath effect is not sensitive to the link environment there.

Table 8.4: Average throughput improvement of SISO links for NEC-AP.

field	AP	1) original (Mbps)	2) before (Mbps)	imp. rate from 1) (%)	3) after (Mbps)	imp. rate from 2) (%)
field#1	AP1	51.06	65.23	27.75	65.23	0.00
	AP4	57.90	67.29	16.22	71.18	5.78
field#2	AP1	40.48	52.88	30.66	61.87	16.99
	AP4	49.09	52.17	6.28	69.60	33.42
field#3	AP1	64.26	70.42	9.59	73.39	4.23
	AP5	69.55	78.63	13.06	78.63	0.00

Table 8.5: Average throughput improvement of MIMO links for NEC-AP.

field	AP	1) original (Mbps)	2) before (Mbps)	imp. rate from 1) (%)	3) after (Mbps)	imp. rate from 2) (%)
field#1	AP1	139.63	145.94	4.51	145.94	0.00
	AP4	155.36	179.86	15.77	182.00	1.19
field#2	AP1	141.28	155.59	10.13	160.33	3.05
	AP4	166.00	174.92	5.37	174.92	0.00
field#3	AP1	147.17	156.38	6.26	156.38	0.00
	AP5	161.56	169.43	4.87	171.00	0.93

8.4 Evaluations for Various AP Devices

In this section, we evaluate the proposal through applications to three commercial AP devices from two vendors in the same three fields using MIMO links.

8.4.1 Adopted AP Devices

For evaluations, we adopt Buffalo WZR-1750DHP [60], IO-Data WNAC1600DGR3 [66], and IO-Data WN-AX2033GR [83]. The last device was used only in field#3.

8.4.2 Throughput Results

Tables 8.6 and 8.7 show the average throughput improvements for them. They compare the average throughputs among the same three cases. The results indicate that the coordinate optimization can improve for all the APs except Buffalo-AP1 in field#2 and IO-Data-AP4 in field#1. Specifically, for Buffalo-AP4 in field#1, the average throughput is improved from 168.34 Mbps to 171.64 Mbps, which means 1.96% improvement. For IO-Data-AP1 in field#1, the average throughput is improved from 146.91 Mbps to 154.15 Mbps, which means the 4.93% improvement. Thus, it is confirmed that the proposed setup optimization approach improves the throughput performance for various AP devices.

Table 8.6: Average throughput improvement for Buffalo-AP.

field	AP	1) original (Mbps)	2) before (Mbps)	imp. rate from 1) (%)	3) after (Mbps)	imp. rate from 2) (%)
field#1	AP1	144.79	155.85	7.64	158.20	1.51
	AP4	157.94	168.34	6.58	171.64	1.96
field#2	AP1	153.15	171.00	11.66	171.00	0.00
	AP4	165.17	169.48	2.61	170.92	0.85
field#3	AP1	152.04	158.22	4.07	160.80	1.63
	AP5	152.94	155.83	1.89	156.50	0.43

Table 8.7: Average throughput improvement for IO-Data-AP.

field	AP	1) original (Mbps)	2) before (Mbps)	imp. rate from 1) (%)	3) after (Mbps)	imp. rate from 2) (%)
field#1	AP1	136.61	146.91	7.54	154.15	4.93
	AP4	149.31	163.43	9.46	163.43	0.00
field#2	AP1	139.16	144.39	3.76	147.02	1.82
	AP4	149.53	161.75	8.18	164.00	1.39
field#3	AP1	134.25	141.01	5.03	143.89	2.04
	AP5	131.06	133.76	2.06	134.65	0.67

8.5 Summary

In this chapter, we presented the evaluations of the proposed AP setup optimization approach in three network fields. First, we optimized the AP setup by manually changing the orientation and height of the AP to increase the measured throughput between the AP and the corresponding bottleneck host. Then, we investigated the overall throughput improvement among the hosts by the AP setup optimization. The results confirm that AP setup optimization improves the overall throughput for any AP location. In addition, we presented the coordinate shift as another optimization parameter in the AP setup optimization approach. The results confirm that the coordinate shift also improves the overall throughput. Finally, we evaluated the AP setup optimization approach for several commercial AP devices from two vendors in the same three fields using MIMO links. It is confirmed that the proposed setup optimization approach improves the throughput performance for various AP devices.

Chapter 9

Conclusion

In this thesis, we presented the study of the minimax access-point (AP) setup optimization approach for the IEEE 802.11n wireless local-area network (WLAN).

Firstly, we introduced related wireless technologies such as the IEEE 802.11n protocol, the channel bonding, the multiple-input-multiple output (MIMO), antennas in MIMO, and the signal propagation.

Secondly, we presented TCP throughput measurement results using IEEE 802.11n commercial AP devices under various placement heights and orientations in outdoor and indoor environments. The results show that the throughput of the IEEE 802.11n link can be strongly affected by the placement height and the roll angle of the AP.

Thirdly, we proposed the minimax AP setup optimization approach that consists of five steps to improve the network performance. Each AP setup is optimized in terms of the orientation, the height, and the coordinate to maximize the measured throughput between the AP and the corresponding bottleneck host.

Fourthly, we proposed the throughput estimation model for our approach. This model uses the *log-distance path loss model* for the receiving signal strength estimation, and the *sigmoid function* for the throughput estimation. Besides, this model considers the *indirect signal* for the *multipath effect*. The selection procedure of the host locations is also presented to reduce the labor costs in throughput measurements for the parameter optimization of the model.

Fifthly, we offered the *parameter optimization tool* to find optimal values of parameters in the throughput estimation model.

Sixthly, we verified the effectiveness of the proposed throughput estimation model with the use of the parameter optimization tool. The accuracy of the throughput estimation model is examined by comparing the estimated throughputs with the measurement results in three network fields. The effectiveness of the host location selection procedure for the model parameter optimization is also evaluated there. The results in SISO links and MIMO links show that the same bottleneck host is found by the model and by the measurements for any AP in the three fields. Thus, the effectiveness of our proposals is confirmed.

Finally, we verified the effectiveness of the proposed AP setup optimization approach through extensive measurements using several commercial AP devices and MIMO links in the three network fields. The results confirm that the proposed approach improved the overall host throughput for any AP location.

In future works, we will apply the minimax AP setup optimization approach for other protocols including IEEE 802.11ac at 5 GHz. We will also extend the throughput estimation model to consider concurrent communications between multiple APs and multiple hosts, while the load bal-

ance between the APs should be considered. The host location selection procedure for the model parameter optimization will also be evaluated in other network fields. Then, these proposals will be applied in various network fields.

Bibliography

[1] M. S. Gast, 802.11wireless networks, 2nd ed., O'Reilly, 2005.

[2] M. S. Gast, 802.11n: a survival guide, 1st ed., O'Reilly, 2012.

[3] H. C. Lo, D. B. Lin, T. C. Yang, and H. J. Li, "Effect of polarization on the correlation and capacity of indoor MIMO channels," Int. J. Antenna. Propagation, 2012.

[4] D. Kong, E. Mellios, D. Halls, A. Nix, and G. Hilton, "Throughput sensitivity to antenna pattern and orientation in 802.11 n networks," Indoor. Mob. Radio Commun., pp. 809-813, Sept. 2011.

[5] Z. Sun and I. Akyildiz, "Channel modeling and analysis for wireless networks in underground mines and road tunnels," IEEE Trans. Commun., vol. 58, no. 6, pp. 1758-1768, 2010.

[6] P. Y. Qin, Y. J. Guo, and C. H. Liang, "Effect of antenna polarization diversity on MIMO system capacity," Proc. IEEE Antenna. Wireless Propagation, Vol. 9, pp.1092-1095, 2010.

[7] A. N. Gonzalez and B. Lindmark, "The effect of antenna orientation and polarization on MIMO capacity," Proc. IEEE Int. Symp. Antenna. Propagation, vol. 3, pp. 434-437, 2005.

[8] O. Klemp and H. Eul, "Radiation pattern analysis of antenna systems for MIMO and diversity configurations," Advances in Radio Science, vol.3, pp.157-165, 2005.

[9] P. S. Kildal and K. Rosengren, "Correlation and capacity of MIMO systems and mutual coupling, radiation efficiency, and diversity gain of their antennas: simulations and measurements in a reverberation chamber," IEEE Comm. Mag., vol. 42, no. 12, pp.104-12, Dec. 2004.

[10] P. Kyritsi, D. C. Cox, and R. A.Valenzuela, "Effect of antenna polarization on the capacity of a multiple element system in an indoor environment," IEEE Journal on Selected areas in Communications, vol. 20, no. 6, pp. 1227-1239, 2002.

[11] T. Svantesson and A. Ranheim, "Mutual coupling effects on the capacity of multielement antenna systems," Proc. (ICASSP'01), IEEE Int. Conf., Vol. 4, pp. 2485-2488, 2001.

[12] J. P. Kermoal, L. Schumacher, P. E. Mogensen, and K. I. Pedersen, "Experimental investigation of correlation properties of MIMO radio channels for indoor picocell scenarios," IEEE-VTS Fall VTC 52nd, Vol. 1, pp.14-21, 2000.

[13] K. S. Lwin, N. Funabiki, Md. E. Islam, C. C. Chew, and Y. Tani, "Throughput measurements in outdoor environment with different AP placement heights and orientations for IEEE 802.11n wireless networks," Proc. IEEE Hiroshima Section Student Symp., pp. 406-409, Nov. 2015.

[14] K. S. Lwin, N. Funabiki, and Md. E. Islam, "Throughput measurements with various indoor AP placement conditions for IEEE 802.11n wireless networks," Proc. IEICE General Conf., BS-3-35, March 2016.

[15] N. Funabiki, K. S. Lwin, M. Kuribayashi, and I. W. Lai, "Throughput measurements for access-point installation optimization in IEEE 802.11n wireless networks," Proc. IEEE ICCE-TW, pp. 218-219, May 2016.

[16] K. S. Lwin, N. Funabiki, K. K. Zaw, M. S. Al Mamun, and M. Kuribayashi, "Throughput measurements for access-point setup optimization in IEEE802.11n wireless networks," IEICE Tech. Rep., vol.116, no.146, pp. 27-32, July 2016.

[17] K. S. Lwin, N. Funabiki, K. K. Zaw, M. S. A. Mamun, and M. Kuribayashi, " A minimax approach for access-point setup optimization using throughput measurements in IEEE 802.11n wireless networks," Proc. Int. Symp. Comput. Networking, pp. 311-317, Nov. 2016.

[18] K. S. Lwin, N. Funabiki, C. Taniguchi, K. K. Zaw, M. S. A. Mamun, M. Kuribayashi, and W.-C. Kao, "A minimax approach for access point setup optimization in IEEE 802.11n wireless networks," Int. J. Netw. Comput., vol. 7, no. 2, pp. 187-207, July 2017.

[19] K. S. Lwin, N. Funabiki, S. K. Debnath, and M. K. Ismael "A minimax approach for access-point setup optimization in IEEE 802.11n WLAN with MIMO links," Proc. IEEE Hiroshima Section Student Symp., pp. 234-237, Dec. 2017.

[20] D. B. Faria, "Modeling signal attenuation in IEEE 802.11 wireless LANs," Tech. Report, TR-KP06-0118, Stanford Univ., July 2005.

[21] T. Sekioka, N. Funabiki, and T. Higashino, "A proposal of an improved function synthesis algorithm using genetic programming," IEICE Trans. D1, vol. J83-D-I, no.4, pp.407-417, Apr. 2000.

[22] T. Sekioka, Y. Yokogawa, N. Funabiki, T. Higashino, T. Yamada, and E. Mori, "A proposal of a lip contour approximation method using the function synthesis," IEICE Trans. D2, vol. J84-D-II, no.3, pp.459-470, March 2001.

[23] N. Funabiki, C. Taniguchi, K. S. Lwin, K. K. Zaw, and W.-C. Kao, "A parameter optimization tool and its application to throughput estimation model for wireless LAN," Proc. Int. Work. Virtual Environ. Netw.-Orient. Appli., pp. 701-710, July 2017.

[24] K. S. Lwin, K. K. Zaw, and N. Funabiki, "Throughput measurement minimization for parameter optimization of throughput estimation model," Proc. Chugoku-Branchi J. Conf., Oct. 2017.

[25] A. M. Gibney, M. Klepal, and D. Pesch, "A wireless local area network modeling tool for scalable indoor access point placement optimization," Proc. Spring Simulation Multiconf., Society for Computer Simulation International, pp. 163-170, Apr. 2010.

[26] Y. Lee, K. Kim, and Y. Choi, "Optimization of AP placement and channel assignment in WLAN," Proc. IEEE Conf. Local Compu. Netw., pp. 831-836, Nov. 2002.

[27] M. A. Jensen and J. W. Wallace, "A review of antennas and propagation for MIMO wireless communications," IEEE Trans. Antenna. Propagation, vol. 52, no. 11, pp. 2810-2824, Nov. 2004.

[28] W. Zhu, D. Browne, and M. Fitz, "An open access wideband multiantenna wireless testbed with remote control capability," Proc. IEEE Tridentcom, pp. 72-81, Feb. 2005.

[29] D. Piazza, N. J. Kirsch, A. Forenza, R. W. Heath, and K. R. Dandekar, "Design and evaluation of a reconfigurable antenna array for MIMO systems," IEEE Trans. Antenna. Propagation, vol. 56, no. 3, pp. 869-881, March 2008.

[30] A. E. Forooshani, C. T. Lee, and D. G. Michelson, "Effect of antenna configuration on MIMO-based access points in a short tunnel with infrastructure," IEEE Trans. Commun., vol. 64, no. 5, pp. 1942-1951, May 2016.

[31] S. Banerji and R. S. Chowdhury, "On IEEE 802.11: wireless LAN technology," Int. J. of Mobile Net. Comm. & Telematics, vol. 3, no. 4, Aug. 2013.

[32] S. Banerji, "Upcoming standards in wireless local area networks," Wireless & Mobile Technologies, vol. 1, no. 1, Sept. 2013.

[33] I. Poole, "IEEE 802.11 Wi-Fi standards," Internet: http://www.radio-electronics.com/info/wireless/wi-fi/ieee-802-11-standards-tutorial.php, Access May 12, 2018.

[34] V. Beal, "What is 802.11 wireless LAN standards?," Internet: http://www.webopedia.com/TERM/8/802_11.html, Access May 12, 2018.

[35] "IEEE 802.11 - Wikipedia," Internet: http://en.wikipedia.org/wiki/IEEE_802.11, Access May 12, 2018.

[36] C. C. Choon, "A study of active access-point selection algorithm for wireless mesh network under practical conditions," Ph.D. thesis, Grad. School of Natural Science and Technology, Okayama University, Japan, Sept. 2015.

[37] M. E. Islam, "A study of access-point aggregation algorithm for elastic wireless local-area network system and its implementation," Ph.D. thesis, Grad. School of Natural Science and Technology, Okayama University, Japan, March 2016.

[38] S. Sendra, M. Garcia, C. Turro, and J. Loret, "WLAN IEEE 802.11 a/b/g/n indoor coverage and interference performance study," Int. J. Adv. in Netw. and Services, vol. 4, no. 1 and 2, pp. 209-222, 2011.

[39] A. S. Tanenbaum and D. J. Wetherall, Computer Networks, 5th ed., Pearson Prentice Hall, 2011.

[40] J. H. Yeh, J. C. Chen, and C. C. Lee, "WLAN standards," IEEE Potentials, vol. 22, no. 4, 2003.

[41] IEEE, "IEEE Std 802.11-2012, IEEE standard for Information technology-telecommunications and information exchange between systems-local and metropolitan area networks- specific requirements-Part 11: wireless LAN medium access control (MAC) and physical layer (PHY) specifications," Internet: http://standards.ieee.org/getieee802/download/802.11-2012.pdf, Access May 12, 2018.

[42] O. Bejarano, E. W. Knightly, and M. Park, "IEEE 802.11 ac: from channelization to multi-user MIMO," IEEE Comm. Mag., vol. 51, no. 10, pp. 84-90, Oct. 2013.

[43] L. Verma, M. Fakharzadeh, and S. Choi, "Wifi on steroids: 802.11 ac and 802.11 ad," IEEE Trans. Wireless Comm., vol. 20, no. 6, pp. 30-35, Dec. 2013.

[44] M. S. Gast, 802.11ac: a survival guide, 1st ed., O'Reilly, 2013.

[45] M. J. Lopes, F. Teixeira, J. B. Mamede, and R. Campos, "Wi-Fi broadband maritime communications using 5.8 GHz band," Proc. Underwater Commun. Network. (UComms), pp. 1-5, Sept. 2014.

[46] J. Jansons and T. Dorins, "Analyzing IEEE 802.11n standard: outdoor performance," Proc. ICDIPC, pp. 26-30, 2012.

[47] U. Paul, R. Crepaldi, J. Lee, S.-J. Lee, and R. Etkin, "Characterizing WiFi link performance in open outdoor networks," Proc. IEEE SECON, pp. 251-259, 2011.

[48] "WiMAX Page, IEEE802.11ac Works," Internet: http://123-info.net/wimax-page/archives/918, Access May 12, 2018.

[49] L. Deek, E. Garcia-Villegas, E. Belding, S. J. Lee, and K. Almeroth, "The impact of channel bonding on 802.11n network management," Proc. The 7th Conf. on Emerging Netw. Exp. and Tech. (CoNEXT '11), Dec. 2011.

[50] T. D. Chiueh, P. Y. Tsai, and I. W. Lai , "Wireless MIMO-OFDM communications," 2nd ed., Wiley, 2012.

[51] "IEEE 802.11n-2009 - Wikipedia," Internet: http://en.wikipedia.org/wiki/IEEE_802.11n-2009, Access Feb. 26, 2016.

[52] E. Perahia and R. Stacey, Next Generation Wireless LANS: 802.11n and 802.11ac, Cambridge Univ. press, Cambridge, May 2013.

[53] NEC Inc., "WG2600HP manual," Internet: http://www.aterm.jp/support/manual/pdf/am1-002673.pdf, Access Feb. 1, 2016.

[54] D. Kong, E. Mellions, D. Halls, A. Nix, and G. Hilton, "Throughput sensitivity for antenna pattern and orientation in 802.11n networks," Proc. IEEE 22nd Int. Symp. Indoor. Mob. Radio Commun., pp. 809-813, Sept. 2011.

[55] H. C. Lo, D. B. Lin, T. C. Yang, and H. J. Li, "Effect of polarization on the correlation and capacity of indoor MIMO channels," Int. J. Antenna. Propagation, 2012.

[56] Cisco Systems Inc.,"Antenna patterns and their meaning," White Paper, 2007, Internet: http://www.cisco.com/c/en/us/products/collateral/wireless/aironet-antennas-accessories/prod_white_paper0900aecd806a1a3e.pdf, Access Sept. 23, 2016.

[57] D. Hucaby, CCNP BCMSN Exam Certification Guide, 4th ed., Cisco Press, 2007.

[58] M. F. Iskander and Z. Yun, "Propagation prediction models for wireless communication systems," IEEE Trans. on microwave theory and techniques, Vol.50, no. 3, pp. 662-673, 2002.

[59] S. Rackley, Wireless Networking Technoloty, Newnes Publishing, 2007.

[60] Buffalo Inc., "AirStation WZR-1750DHP user manual," Internet: http:manual.buffalo.jp/buf-doc/35013154-01_EN.pdf, Access Oct. 3, 2015.

[61] Speed Guide Inc., SG TCP Optimizer, Internet: http://www.speedguide.net/sg_tools.php, Access Oct. 3, 2015.

[62] WiFi Channel Scanner, Internet: http://www.wifichannelscanner.com/index.html, Access Oct. 3, 2015.

[63] ACD.net, Iperf Speed Testing, Internet: http://support.acd.net/wiki/index.php?title=IperfSpeedTesting, Access Oct. 3, 2015.

[64] Japan Meteorology Agency, Internet: http://www.data.jma.go.jp/obd/stats/etrn/index.php, Access Oct. 3, 2015.

[65] C. C. Chew, N. Funabiki, T. Nakanishi, and K. Watanabe, "Throughput measurements using IEEE802.11n and 11ac devices for high-speed wireless networks," Proc. Chugoku-branch Joint Con. Inst. Elect. Inform. Eng., pp. 232-233, 2013.

[66] IO data Inc., Internet: http://www.iodata.jp/product/network/wnlan/wn-ac1600dgr3/index.htm, Access Feb. 1, 2016.

[67] G. Wölfle, R. Wahl, P. Wertz, P. Wildbolz, and F. Landstorfer, "Dominant path prediction model for indoor scenarios," Proc. German Microwave Conf. (GeMIC), vol. 27, Apr. 2005.

[68] D. Plets, W. Joseph, K. Vanhecke, E. Tanghe, and L. Martens, "Coverage prediction and optimization algorithms for indoor environments," EURASIP J. Wireless Comm. Netw., no.1, pp. 1-23, Dec. 2012.

[69] Y. A. S. Dama, R. A. A. Alhameed, F. S. Quinonez, D. Zhou, S. M. R. Jones, and S. Gao, "MIMO indoor propagation prediction using 3D shoot-and-bounce ray (SBR) tracing technique for 2.4 GHz and 5 GHz," Proc. IEEE European Conf. (EUCAP), pp. 1655-1658, 2011.

[70] Funabiki N., ed., "Wireless mesh networks," InTech-Open Access Pub., Jan. 2011, Internet: http://www.intechopen.com/books/wireless-mesh-networks, Access Jan. 20, 2017.

[71] ns-3, Internet: https://www.nsnam.org, Access Jan. 20, 2017.

[72] A. Alhamoud, M. Kreger, H. Afifi, C. Gottron, D. Burgstahler, F. Englert, D. Böhnstedt, and R. Steinmetz, "Empirical investigation of the effect of the door's state on received signal strength in indoor environments at 2.4 GHz," Proc. IEEE 39th Conf. Comp. Netw., pp. 652-657, Sept. 2014.

[73] T. K. Sarkar, Z. Ji, K. Kim, A. Medour, and M. S. Palma, "A survey of various propagation models for mobile communication," IEEE Antenna. propagation Mag., vol. 45, no. 3, pp. 51-82, June 2003.

[74] D. Xu, Z. Jianhua, G. Xinying, Z. Ping, and W. Yufei, "Indoor office propagation measurements and path loss models at 5.25 GHz," Proc. IEEE 66th Vehicular Technology Conf. (VTC), pp. 844-848, 2007.

[75] K. W. Cheung, J. M. Sau, and R. D. Murch, "A new empirical model for indoor propagation prediction," IEEE Trans. Vehicular Technology, vol. 47, no. 3, pp. 996-1001,1998.

[76] Software Verzeichnis development, Homedale WLAN Monitor, Internet: http://www.the-sz.com/products/homedale, Access Feb. 15, 2017.

[77] M. E. Islam, K. S. Lwin, M. A. Mamum, N. Funabiki, and I. W. Lai, "Measurement results of three indices for IEEE 802.11n wireless networks in outdoor environments," Proc. IEEE Hiroshima Section Student Symp., pp. 410-414, Nov. 2015.

[78] R. Akl, D. Tummala, and L. Xinrong, "Indoor propagation modeling at 2.4 GHz for IEEE 802.11 networks," Proc. Sixth IASTED Int. Multi-Conf. Wireless. Optical Commun., July 2006.

[79] K. Farkas, Á. Huszák, and G. Gódor, "Optimization of Wi-Fi access point placement for indoor localization," Network. Commun., vol. 1, no. 1, pp. 28-33, July 2013.

[80] R. F. Safna, E. J. N. Manoshantha, S. A. T. S. Suraweera, and M. B. Dissanayake, "Optimization of wireless pathloss model JTC for access point placement in wireless local area network," Proc. RSEA, pp. 235-238, 2015.

[81] M. S. A. Mamun, M. E. Islam, N. Funabiki, M. Kuribayashi, and I-W. Lai, "An active access-point configuration algorithm for elastic wireless local-area network system using heterogeneous devices," Int. J. Network. Comput., vol. 6, no. 2, pp. 395-419, July 2016.

[82] S. K. Debnath, M. Saha, N. Funabiki, and W. Kao, "A Throughput Estimation Model for IEEE 802.11n MIMO Link in Wireless Local-Area Networks," to appear in 3rd Int. Conference on Computer and Communication Systems (ICCCS 2018).

[83] IO data Inc., Internet: http://www.iodata.jp/product/network/wnlan/wn-ax2033gr/index.htm, Access Feb. 10, 2018.